Towards understanding the cell surface phenotype, metabolic properties and immune functions of resident macrophages of the peritoneal cavity and splenic red pulp using high resolution quantitative proteomics

Nagala, Manjula; Crocker, Paul R.

Published in:
Wellcome Open Research

DOI:
10.12688/WELLCOMEOPENRES.16061.1

Publication date:
2020

RESEARCH ARTICLE

Towards understanding the cell surface phenotype, metabolic properties and immune functions of resident macrophages of the peritoneal cavity and splenic red pulp using high resolution quantitative proteomics [version 1; peer review: 1 approved, 1 approved with reservations]

Manjula Nagala, Paul R. Crocker

School of Life Sciences, University of Dundee, Dundee, DD1 5EH, UK

v1 **First published:** 08 Jul 2020, **5**:165
https://doi.org/10.12688/wellcomeopenres.16061.1
Latest published: 08 Jul 2020, **5**:165
https://doi.org/10.12688/wellcomeopenres.16061.1

Abstract

Background: Resident macrophages (Mϕs) are distributed throughout the body and are important for maintaining tissue homeostasis and for defence against infections. Tissue Mϕs are highly adapted to their microenvironment and thought to mediate tissue-specific functions involving metabolism and immune defence that are not fully elucidated.
Methods: We have used high resolution quantitative proteomics to gain insights into the functions of two types of resident tissue Mϕs: peritoneal cavity Mϕs and splenic red pulp Mϕs. The cellular expression levels of many proteins were validated by flow cytometry and were consistently in agreement with the proteomics data.
Results: Peritoneal and splenic red pulp macrophages displayed major differences in cell surface phenotype reflecting their adaptation to different tissue microenvironments and tissue-specific functions. Peritoneal Mϕs were shown to be enriched in a number of key enzymes and metabolic pathways normally associated with the liver, such as metabolism of fructose, detoxification, nitrogen homeostasis and the urea cycle. Supporting these observations, we show that peritoneal Mϕs are able to utilise glutamine and glutamate which are rich in peritoneum for urea generation. In comparison, splenic red pulp Mϕs were enriched in proteins important for adaptive immunity such as antigen presenting MHC molecules, in addition to proteins required for erythrocyte homeostasis and iron turnover. We also show that these tissue Mϕs may utilise carbon and nitrogen substrates for different metabolic fates to support distinct tissue-specific roles.
Conclusions: This study provides new insights into the functions of tissue Mϕs in immunity and homeostasis. The comprehensive

Open Peer Review

Reviewer Status ? ✓

	Invited Reviewers	
	1	**2**
version 1 08 Jul 2020	? report	✓ report

1. **Camille Bleriot**, Singapore Immunology Network (SIgN), Singapore, Singapore
Florent Ginhoux, Singapore Immunology Network (SIgN), Singapore, Singapore

2. **Luca Cassetta**, University of Edinburgh, Edinburgh, UK
Jeffrey Pollard, University of Edinburgh, Edinburgh, UK

Any reports and responses or comments on the article can be found at the end of the article.

proteomics data sets are a valuable resource for biologists and immunologists.

Keywords
Macrophage, proteomics, metabolism, immunity, peritoneal cavity, spleen

Corresponding author: Paul R. Crocker (p.r.crocker@dundee.ac.uk)

Author roles: Nagala M: Conceptualization, Data Curation, Formal Analysis, Investigation, Methodology, Software, Visualization, Writing – Original Draft Preparation, Writing – Review & Editing; **Crocker PR**: Conceptualization, Funding Acquisition, Project Administration, Supervision, Writing – Original Draft Preparation, Writing – Review & Editing

Competing interests: No competing interests were disclosed.

Grant information: This work was supported by Wellcome [103744, Wellcome Trust Investigator Award to P.R.C.; 097045, to the University of Dundee Proteomics Facility; 097418, to the Flow Cytometry and Cell Sorting Facility at the University of Dundee].
The funders had no role in study design, data collection and analysis, decision to publish, or preparation of the manuscript.

How to cite this article: Nagala M and Crocker PR. **Towards understanding the cell surface phenotype, metabolic properties and immune functions of resident macrophages of the peritoneal cavity and splenic red pulp using high resolution quantitative proteomics [version 1; peer review: 1 approved, 1 approved with reservations]** Wellcome Open Research 2020, **5**:165 https://doi.org/10.12688/wellcomeopenres.16061.1

First published: 08 Jul 2020, **5**:165 https://doi.org/10.12688/wellcomeopenres.16061.1

Introduction

Resident macrophages (Mϕs) are distributed in tissues throughout the body and contribute to both homeostasis and defence against infectious disease. Resident Mϕs from different tissues are highly heterogeneous in properties and functions and this is reflected in considerable diversity in their transcriptomes[1]. Tissue Mϕs arise from both embryonic and adult sources including yolk sac, foetal liver and bone marrow and recent studies have shown that local signalling within tissues is sufficient to promote the acquisition of specialized Mϕ functions irrespective of their tissue of origin[2]. Therefore, tissue Mϕs have distinct phenotypic and metabolic characteristics that define tissue-specific functions and unique roles, even at steady-state. The detailed molecular characterisation of tissue Mϕs is important in order to fully understand the various roles they play in a given tissue.

Important insights into Mϕ functions have been gained by system-wide analyses of transcriptional regulation and epigenetics[1,3,4]. However, much less is known about protein dynamics. The proteome can differ significantly from the transcriptome due to a variety of regulatory processes such as post-transcriptional processing and degradation of mRNA and protein modifications and degradation, all of which are important in controlling steady-state protein abundance. Recent technological advances in mass spectrometry (MS) permit the systematic quantification of thousands of proteins from cellular lysates[5].

Proteomics data, when combined with complementary approaches, such as bioinformatics and pathway data analysis tools, provides the contextual information required to decode large data sets into meaningful biologically adaptive processes such as cellular functions and metabolic pathways.

Tissue Mϕs can be divided into two categories: those that are 'fixed' within the tissue by being firmly embedded in neighbouring stroma and those that are 'free' to migrate within tissues. To investigate tissue Mϕ proteomes of each category, we selected splenic red pulp Mϕs (SRPM) as an example of fixed Mϕs and peritoneal cavity Mϕs (PM) as an example of free Mϕs[6]. Both of these Mϕ populations are embryo-derived and have some well-known functions. SRPM are important for clearance of aged red blood cells, and iron homeostasis and recycling from senescent and damaged erythrocytes[2,7–9]. In contrast, PM play a role in B1 cell class switching and through their ability to rapidly migrate into visceral organs, they have been shown to play role in tissue repair and liver regeneration[10–15].

To characterise and investigate other possible tissue-specific functions for SRPM and PM at steady-state, we used MS approaches to obtain accurate quantification of protein copy number per cell that was validated by flow cytometry. Comparisons of the proteomes with the corresponding transcriptomes were made using the ImmGen[16] gene expression database, which provided high-throughput validation for the translation of mRNA to protein for many of the differentially expressed genes and also revealed numerous examples of discordance between mRNA and protein levels. We have combined proteomics with complementary approaches, decoded large data sets and revealed novel functions relating to metabolism and host defence, in addition to previously characterised functions.

Methods

Reagents and antibodies

Dulbecco's phosphate buffered saline (PBS) without Ca & Mg, Foetal Bovine Serum (FBS) (qualified, heat inactivated, E.U.-approved), Pen-Strep, Trypsin-EDTA solution, Microplate BCA Protein Assay, sample reducing agent, trypsin protease, Pierce -MS Grade, Roche-COMPLETE Mini EDTA-Free Protease Inhibitor tablets, Roche-PHOSS-RO, PhosSTOP™ Trypan blue solution were from Sigma, UK; CD16/CD32 (Fc-receptor block), V500 anti-mouse I-A/I E antibody (clone: M5/114; Cat# 562366) and PE anti-mouse Siglec-F antibody Cat# 552126 were from BD Bioscience, UK; Alexa Fluor 488 anti-mouse CD11b antibody (M1/70) Cat# 53-0112-82, PE-cy7 anti-mouse CD11c antibody (Clone: N418) Cat# 25-0114-82, PE anti-mouse CD163 antibody (TNKUPJ) Cat# 12-1631-80 were from ThermoS eBioscience™, UK; FITC anti-human/mouse CD49f (ITGA6) antibody Cat# 313605, PE anti-mouse CD51 ITGAV antibody Cat# 104105, Alexa Fluor® 488 anti-mouse CD31 (pecam-1) antibody Cat# 102413, FITC anti-mouse CD66a (CEACAM1a) antibody Cat# 134517, Alexa Fluor® 488 anti-mouse CD102 (ICAM2) antibody Cat# 105609, Alexa Fluor® 488 anti-mouse CD54 (icam1) antibody Cat# 116111, FITC anti-mouse CD200R (OX2R) antibody Cat# 123909, FITC anti-mouse CD244.2 antibody Cat# 133503, FITC anti-mouse CD20 antibody Cat# 150407, PE anti-mouse CD282 (TLR2) antibody Cat# 148603, Alexa Fluor® 488 anti-mouse CD172a (SIRPα) antibody Cat# 144023, Alexa Fluor® 488 anti-mouse F4/80 antibody Cat# 123119, FITC anti-mouse/human CD44 antibody Cat# 103021, APC anti-mouse F4/80 antibody Cat# 123116, APC anti-mouse CD106 antibody Cat# 105717, PE anti-mouse CD80 antibody (16-10A1) Cat# 104707, PE anti-mouse CD86 (B7-2) antibody Cat# 12-0862-82, APC anti-mouse Tim-4 antibody Cat# 130010, PE/Cy7 anti-mouse TLR4 antibody Cat# 117609 were from Biolegend, UK.

Animals

C57BL/6J wildtype mice were used throughout. All 60 mice used in the study were maintained in the Biological Resource Unit at the University of Dundee under specific-pathogen-free conditions following procedures that were approved by the University of Dundee Ethical Committee and under the authorization of the UK Home Office Animals (Scientific Procedures) Act 1986. Mice were housed in same sex groups, in individually ventilated cages and were given standard diet RM3 (SDS Special Diet Services). Housing conditions were: 12-h light, 12-h dark cycle, 21°C temperature and relative humidity of 45–60%. Mice had free access to autoclaved drinking water and autoclaved food *ad libitum*. Mice were humanely killed using a Schedule 1 method of gradual exposure to carbon dioxide and death was confirmed by cervical dislocation.

SRPM isolation and purification

SRPM were purified as described previously[17]. In brief, single cell suspensions of splenocytes were obtained by digesting the

tissue with 400 U/ml collagenase D and 50 µg/ml DNAse 1 at 37°C for 20 minutes, erythrocytes were lysed and passed through a 100 µm cell strainer following suspension in MACS buffer. The single cell suspensions of splenocytes were then passed over LS separation columns (Miltenyi) without further treatment. Before being removed from the magnet, the columns were washed three times with 2 ml MACS buffer (Miltenyi). After removal of the magnet, SRPM were eluted from the separation column with 5 ml MACS buffer and subjected to fluorescence activated cell sorting.

PM Isolation and purification

The peritoneal cavity was flushed with 4–5 ml PBS + 1% FBS + 2 mM EDTA. After centrifugation, cells were resuspended in RPMI medium supplemented with 4 mM L-glutamine, 100 units/ml penicillin, 100 µg/ml streptomycin and 10% heat inactivated FBS and subjected to fluorescence activated cell sorting.

Flow cytometry

Single-cell suspensions were Fc-receptor-blocked for 30 min at 4°C with rat anti-mouse CD16/CD32 antibody in PBS with 1% FBS. Blocked cells were subsequently incubated with fluorophore-conjugated surface-staining primary antibodies for 60 min at 4°C, prior to washing in PBS containing 1% FBS and 2 mM EDTA. Following surface staining, cells were washed and analysed using a Canto II flow cytometer and FlowJo software version 10.0. Raw data for flow cytometry analysis are available, see *Underlying data*[18].

Fluorescence activated cell sorting

Following isolation from the spleen and peritoneal cavity as described above, cells were stained for the Mϕ lineage marker, F4/80 and viability dye DAPI, under sterile conditions. Briefly, cells were pelleted and incubated sequentially with 1:100 Fc-receptor block for 10 min at 4°C, followed by Mϕ marker F4/80 antibody (1:200) and Siglec-F PE antibody (1:200) for 30 min at 4°C. Cells were washed and sorted into F4/80 APC-high-expressing single positive populations on a BD InfluxTM cell sorter into RPMI media containing 20% FBS. Sorted cells were pelleted and processed for proteomics.

Urea assay

Magnetically sorted PM were seeded at 0.25×10^6 cells per well (96-well) in HBSS with 0.5 µM retinoic acid 20 ng/ml M-CSF and incubated for 2 h. The medium was removed and replaced with HBSS with 0.1% BSA with or without 2 mM glutamine and glutamate (+ 0.5 µM retinoic acid, + 20 ng/ml M-CSF), with or without 25 mM glucose. For urea measurements, the supernatant was transferred to fresh 96-well plate after overnight incubation and urea levels were measured using a QuantiChromTM Urea Assay Kit. Raw data for urea quantification are available, see *Underlying data*[18].

Filter-aided sample preparation (FASP) of samples

A total of n=4 biological replicates for PM and n=3 biological replicates for SRPM were processed for proteomic analysis. Cell pellets were solubilised in 100 mM Tris HCl containing 4% SDS, and 100 mM dithiothreitol in the presence of protease and phosphatase inhibitors. Samples were processed using the FASP protocol[19] with some modifications. After removal of SDS with 8 M urea and alkylation with iodoacetic acid, Vivacon 500, 10k MWCO HY filters (Sartorius Stedim Biotech, VN01H22) were washed three times with 100 mM Tris-HCl pH 8 then another four times with 100 mM triethyl ammonium bicarbonate (TEAB). Proteins on the filters were then digested twice at 30°C with trypsin (Pierce) (2 x 2 µg), first overnight and then for another 6 h in a final volume of 200 µl, 100 mM TEAB. The resulting tryptic peptides were desalted using C18 solid phase extraction cartridges (Empore, Agilent technologies) and quantified using the Pierce Quantitative Colorimetric Peptide Assay (Thermo Scientific). Raw data for peptide quantification are available, see *Underlying data*[18].

High pH reverse phase fractionation

Peptides (8 µg for each sample) were dissolved in 200 µL ammonium formate (10 mM, pH 9.5) and fractionated using RP-High pH HPLC. A C18 Column from Waters (XBridge peptide BEH, 130Å, 3.5 µm 2.1 X 150 mm, Ireland) with a guard column (XBridge, C18, 3.5 µm, 2.1X10mm, Waters) are used on a Ultimate 3000 HPLC (Thermo-Scientific). Buffers A and B used for fractionation consist, respectively, of 10 mM ammonium formate in milliQ water and 10 mM ammonium formate with 90% acetonitrile. Both buffers were adjusted to pH 9.5 with ammonia. Fractions were collected using a WPS-3000FC auto-sampler (Thermo-Scientific) at 1 min intervals. Column and guard column were equilibrated with 2% buffer B for 20 min at a constant flow rate of 0.2 ml/min. Samples (180 µl) were loaded onto the column at 0.2 ml/min, and separation gradient start 1 min after sample loading onto the column. Peptides were eluted from the column with a gradient of 2% to 5% buffer B over 6 min and then from 5% to 60% buffer B over 53 min. The column was washed for 16 min in 100% buffer B and equilibrated in 2% buffer B for 20 min as mentioned above. Fraction collection began 1 min after injection and stopped after 80 min (total of 80 fractions, 200 µl each). The total number of fractions concatenated was set to 10 and the content of the fractions was dried and suspended in 50 µl 1% formic acid prior to analysis with LC-MS.

LC-MS analysis

Analysis of peptides was performed on a Velos-Pro (Thermo Scientific) mass spectrometer coupled with a Dionex Ultimate 3000 RS (Thermo Scientific). LC buffers were the following: buffer A (2% acetonitrile and 0.1% formic acid in Milli-Q water (v/v)) and buffer B (80% acetonitrile and 0.08% formic acid in Milli-Q water (v/v). Aliquots of 15 µL of each sample were loaded at 5 µL/min onto a trap column (100 µm × 2 cm, PepMap nanoViper C18 column, 5 µm, 100 Å, Thermo Scientific) equilibrated in 98% buffer A. The trap column was washed for 6 min at the same flow rate and then the trap column was switched in-line with a Thermo Scientific, resolving C18 column (75 µm × 50 cm, PepMap RSLC C18 column, 2 µm, 100 Å). The peptides were eluted from the column at a constant flow rate of 300 nl/min with a linear gradient from 5% buffer B to 35% buffer B in 124 min, and then to 98% buffer B by

126 min. The column was then washed with 98% buffer B for 20 min and re-equilibrated in 98% buffer A for 17 min. Fractions (10) from each sample were analysed using LTQ-Orbitap Velos Pro in data dependent mode. A scan cycle comprised MS1 scan (m/z range from 335–1800) in the Velos orbitrap followed by 15 sequential dependent MS2 scans (the threshold value was set at 5000 and the minimum injection time was set at 200 ms) in LTQ with collision induced dissociation (CID). The resolution of the Orbitrap Velos was set at to 60,000. To ensure mass accuracy, the mass spectrometer was calibrated on the first day that the runs were started.

Proteomics quantification and bioinformatics analysis

A total of n=4 biological replicates for PM and n=3 biological replicates for splenic red pulp Mϕs were subjected to proteomic analysis. The raw mass spectrometric data were processed, searched and quantified using MaxQuant 1.5.5.1[20] and Andromeda as the search engine software[21]. Enzyme specificity was set to that of trypsin/P, allowing for cleavage of N-terminal to proline residues and between aspartic acid and proline residues. Other parameters used were: variable modifications- methionine oxidation, protein N-acetylation; fixed modifications, cysteine carbamidomethylation; database: Uniprot - mouse; minimum peptide length, 7; maximum missed cleavages, 2; PSM & protein false discovery rate, 1%. Default MaxQuant settings included a mass tolerance of 7 ppm for precursor ions, and a tolerance of 0.5 Da for fragment ions. A reverse database was used to apply a maximum false positive rate of 1% for both peptide and protein identification. This cut-off was applied to individual spectra and whole proteins in the MaxQuant output. The match between runs feature was activated with default settings. For bioinformatic and statistical analysis, Perseus software (version 1.5.1.6) was used, all 'Contaminant', 'Reverse' & 'Only identified by site' proteins were removed from the data and the proteomic ruler[5] was used to calculate copy number per cell. Proteins above 2-fold change [log2(2)=1], proteins with nominal p-value less than 0.05 [-log10(0.05)=1.301] were considered as differentially expressed proteins. All bioinformatics, statistical and pathway analyses were performed with the Perseus software[20–22] and Excel was used for basic data analysis and plots. The proteome and the ImmGen mRNA data were merged using R studio based on GeneID. Proteomics data are available via ProteomeXchange with identifier PXD019362.

Statistical analysis

Statistical significance was determined using the two-tailed Student's t-test. All experiments were performed at least twice. P values of <0.05 were considered significant. GraphPad prism version 6 or Perseus version 1.5.1.6 were used.

Results and Discussion

Label-free quantitative proteomics experiments were performed to identify differentially regulated proteins in SRPM and PM that might give insights into their tissue-specific functions under steady-state conditions. Following tissue isolation and cell sorting by flow cytometry, Mϕ populations were around 95% pure (Figure 1A). Database searches enabled the identification of more than 7000 protein groups in these cells (*Extended data*, Table 1)[18]. Label-free quantitative intensity of the proteins obtained using MaxQuant software followed a normal distribution for both the SRPM and PM populations[23] (Figure 1C). The intensities were transformed into absolute quantification of copy number per cell, using the proteomic ruler methodology[5]. Copy numbers for proteins from the 3 (SRPM) or 4 (PM) biological replicates showed strong Pearson correlation coefficients. Variability within replicates for a single population was from 0.968 + 0.0005 for SRPM to 0.985 + 0.002 for PM, indicating robustness and reproducibility of our MS-based peptide quantification methods (Figure 1D). Principal component analysis (PCA) of all proteins expressed by the two sorted populations revealed a relatively greater distance between the SRPM and PM (Figure 1E). Volcano plots showing the distribution of fold-change *versus* *p*-values were generated by plotting the t-test p-value against the PM:SRPM ratio of copy number per cell on a logarithmic scale.

We observed a large number of protein IDs that are differentially regulated between the two populations of Mϕs. However, for many *proteins,* the fold increase obtained using copy number per cell correlated with the increase in cell size/volume determined by forward scatter properties in flow cytometry (Figure 1B, F, upper panel). It has previously been noted that PM are larger in size and volume than the SRPM[24]. To avoid the bias that enriched proteins in the PM are due to this increased cell size, in addition to evaluating differentially regulated proteins using absolute copy number, we also evaluated them following normalisation, centring the median across samples (Figure 1F, lower panel)[25]. We used a fold-change of ≥2 and *p* values of ≤0.05 to define differential regulation across biological replicates. Several proteins were differentially expressed by at least 2-fold when SRPM were compared to PM. Overall, these comparisons indicate minimum variability within replicates for a single population and a noticeable diversity between PM and SRPM populations.

Correlation analysis of mRNA and protein abundance

Integrating multiple levels of information is necessary and valuable to fully elucidate complex biological systems[26–28]. In line with this, we integrated our proteomic data sets with the corresponding mRNA data sets from the ImmGen database (http://rstats.immgen.org/DataPage, GSE15907, *Extended data*, Table 2)[18]. This allowed us to gain global understanding of mRNA and protein expression relationships and to identify differentially regulated proteins that are not evident at the transcriptomic level. Further, this integration of heterogeneous data sets, taken from different laboratories and across experimental platforms, has provided high-throughput data validation and effective use of the data to gain insights into complex biological functions of tissue Mϕ populations.

Out of 7533 unique proteins from our proteome data set, we identified 6903 corresponding transcripts from the ImmGen database and used these for correlation analyses (*Extended data,* Table 3)[18]. The results show moderate positive correlations between mRNA and protein abundance for both Mϕ populations (Figure 2A, B). As observed in other studies, improved

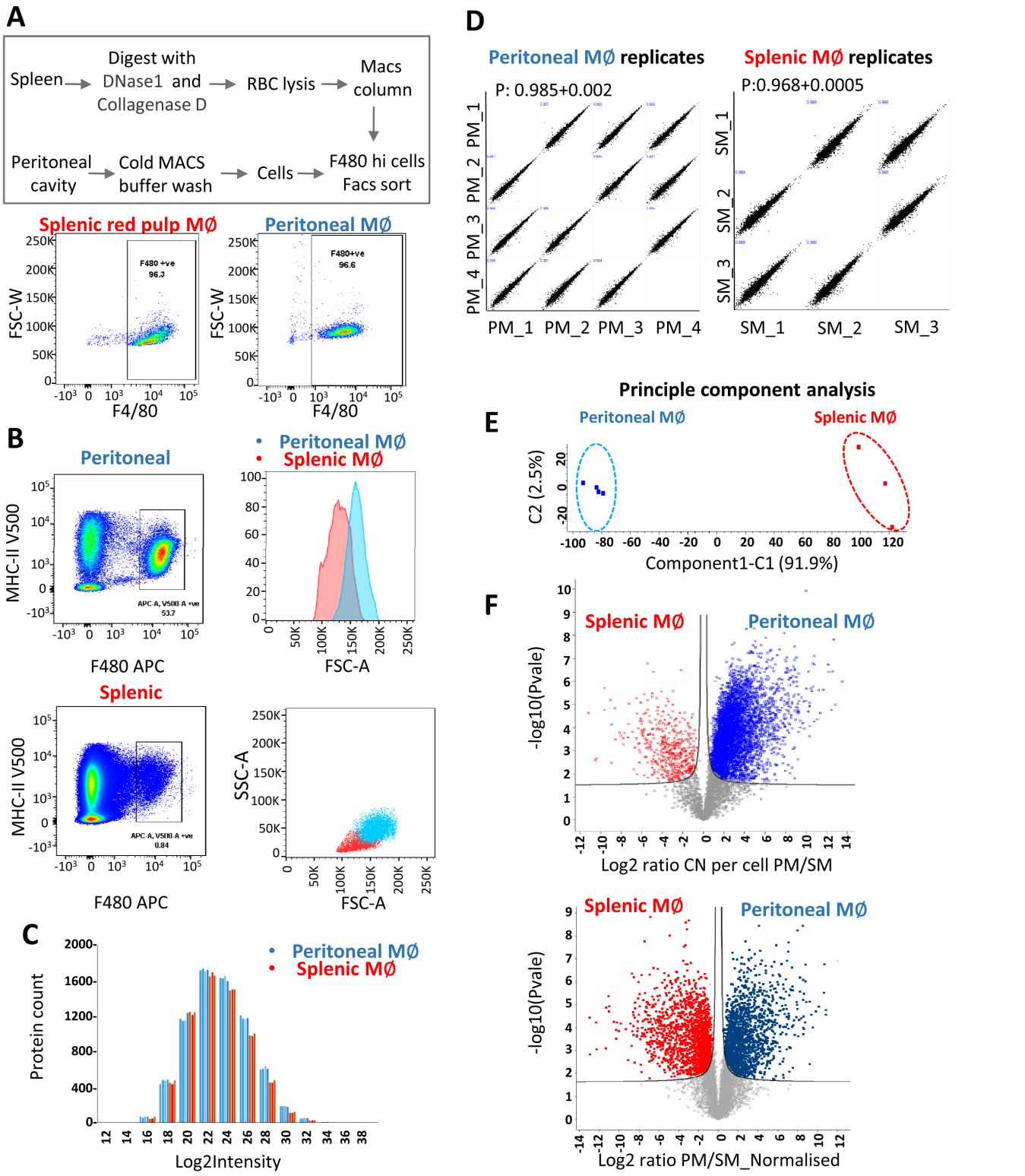

Figure 1. Peritoneal cavity and splenic red pulp macrophage proteomes. (**A**) Schematic overview of procedures used to isolate SRPM and PM (upper panel) and flow cytometry dot plots showing purities of SRPM and PM post FACS (lower panel). (**B**) Flow cytometry plots showing difference in cell size for the F4/80 positive Mϕs gated in peritoneal and splenic cell populations. (**C**) Histogram displaying the distribution of log2-transformed LFQ intensities of indicated samples. (**D**) Scatter plots of estimated protein copy numbers using the proteomic ruler approach show high correlation for biological replicates as indicated by the coefficient of determination being close to 1. (**E**) PCA scores plot showing clustering of proteins according to tissue specific Mϕ samples. (**F**) Volcano plots showing fold changes in proteins using copy number vs. log-transformed P-values from mass spectrometry analysis of PM and SRPM proteomes. Lower panel shows normalization, centering on the median. Four biological replicates for PM and three biological replicates for SRPM were used.

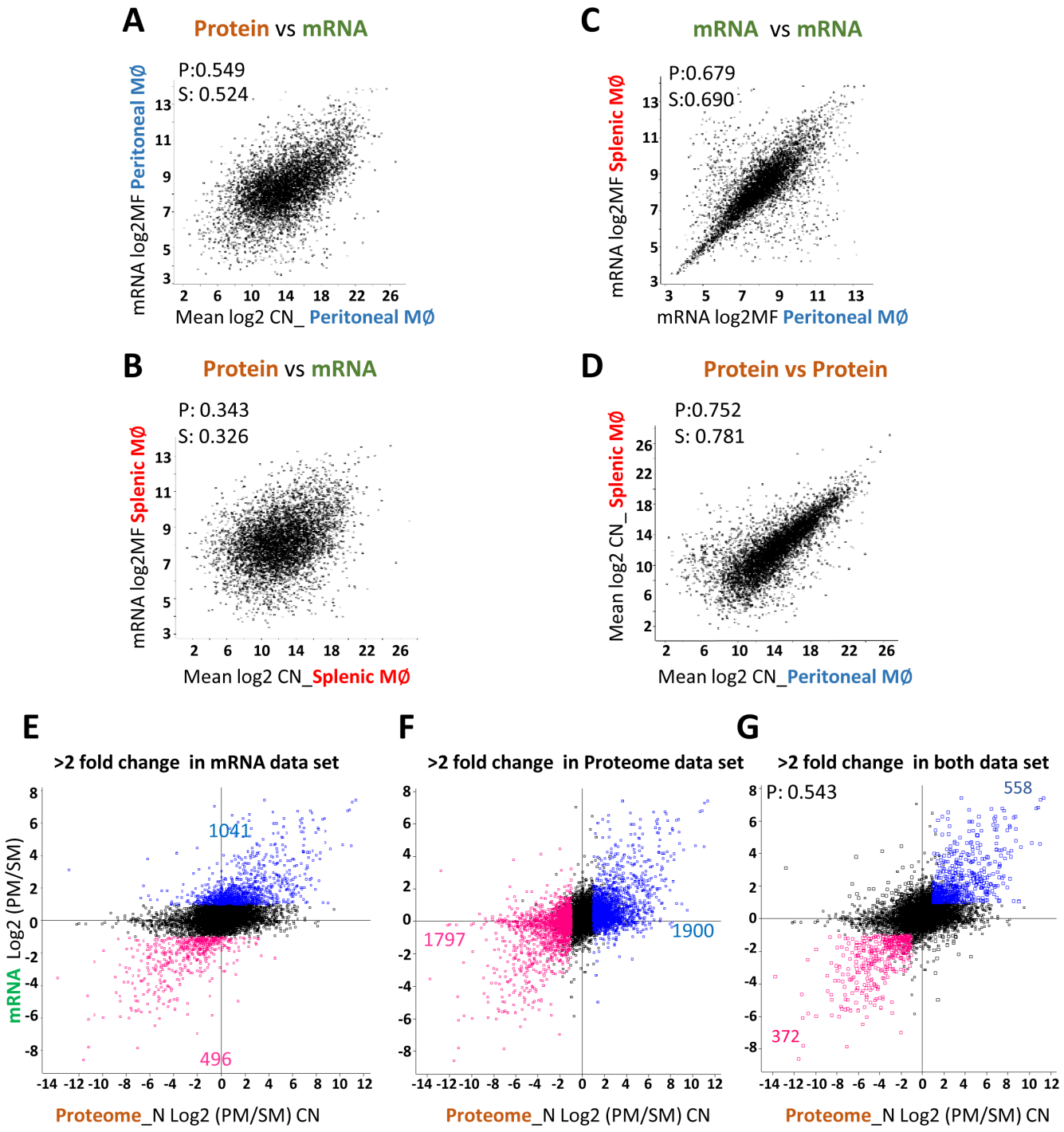

Figure 2. Correlation between the transcriptome and the proteome. Scatter plots based on mean protein copy number for the proteome data set and mean fluorescence for the mRNA data set. (**A**) Correlation of protein vs mRNA for PM data sets; (**B**) correlation of protein vs mRNA for SRPM data sets; (**C**) correlation of PM mRNA vs SRPM mRNA and (**D**) correlation of PM proteins vs SRPM proteins from the proteome data. (**E**, **F**, **G**) Scatter plots of fold changes obtained using mRNA data vs fold changes obtained using proteome data. The coloured dots indicate differentially expressed genes that were statistically significant in the mRNA data set (**E**), protein data set (**F**), or both (**G**). The proteomics data were derived from 4 (PM) or 3 (SRPM) biological replicates. The mRNA data were derived from 3 biological replicates for each Mϕ population.

correlations were observed when PM mRNA was compared with SRPM mRNA or when the PM proteome was correlated with the SRPM proteome (Figure 2, D)[29]. This can be explained in part by fundamental limitations and differences in transcript and protein behaviour, with mRNA half-life ranging from 0.1 to ~40 h versus protein half-life 0.5 to >500 h[30,31]. On the one hand, when a target protein reaches saturating levels, gene silencing or transcript degradation pathways may predominate, leading to an inverse or moderate correlation. On the other hand, when a target protein is in demand in the cell, protein synthesis and mRNA expression may display a strong correlation.

Next, we asked whether transcripts that showed tissue-specific enrichment, based on ImmGen microarray analysis, were similarly enriched at the protein level. The mRNA data set has 1537 unique transcripts that are differentially and significantly regulated (Figure 2E), compared to 3697 unique proteins in the proteomic dataset (Figure 2F). Correlation analysis showed that 930 distinct transcripts (that have tissue-specific enrichment) were positively correlated with their corresponding proteins from the proteome data set (Figure 2G and *Extended data*, Table 4)[18]. However, we noticed that more than 35% of the differentially regulated transcripts were not correlated. This may be due to fundamental biological differences in transcript and protein behaviour or regulatory programs as discussed above, as well as variability associated with the global measurement of transcripts and proteins, such as differences in sensitivity, dynamic range, with the proteome being more dynamic (Figure 2A, B: X axis, proteome; Y axis, mRNA). In conclusion, our correlation of mRNA and protein abundance provides cross-platform/laboratory comparisons and high throughput validation for the translation of mRNA to protein for many of the differentially expressed genes. This correlation analysis also identified numerous examples of mismatches between mRNA and protein expression. The proteomes have thus provided many additional novel insights concerning the biology of these Mϕ populations not observed at the mRNA level.

Characterization and validation of common and tissue specific membrane proteins: novel insights not evident from the transcriptome

Cell surface proteins play a critical role in sensing and responding to the tissue microenvironment and are commonly expressed differentially amongst leukocyte subsets. Proteomic data showed that the cell adhesion molecules (CAMs) VCAM1, F11R (JAM1), CADM1 and PECAM1 were expressed exclusively in SRPM, whereas ICAM2, NINJ1, BCAM, CEACAM1 and ALCAM were expressed specifically by PM, with the first two being the major adhesion receptors (Figure 3A). Adhesion receptor ICAM1 was expressed at similar levels in both the Mϕ populations.

Integrins are a large family of heterodimeric adhesion receptors that contain an α- and a β- subunit. The β2 integrins exhibited striking differential expression, with CD11b (ITGAM α-chain; ITGB2 β-chain) being dominant on PM, but CD11d (ITGAD α-chain; ITGB2 β-chain) being exclusively expressed by SRPM (Figure 3B). PM expressed higher levels of ITGA6 (α6-chain) and ITGA4 (α4-chain) which pair with β1 and either β1 or β7, respectively. ITGAV (αV-chain), which can pair with several β chains, was expressed at similar levels on PM and SRPM. The quantitative proteomics further showed that the integrin α- and β-chains were in 1:1 stoichiometry in each case (interconnecting arrows, Figure 3B).

Many of the adhesion molecules identified by proteomics were validated by flow cytometry, showing an excellent correlation between proteomics data and transcriptome data (Figure 3C). The observed tissue specific expression of CAMs and integrins suggest that many of these adhesion molecules have roles in tissue specific interactions[32].

Next we assessed Mϕ expression of Toll-like receptors (TLRs), which play a key role in the innate immune system. The proteomic analysis showed enrichment of TLR2 and TLR13 in PM and TLR9 in SRPM. Other TLRs were expressed at similar levels in both tissue Mϕs (Figure 3A and Figure 4A, B). The proteomics data were in disagreement with the transcriptome data for TLR2 expression (Figure 4A), but its preferential expression in PM shown by proteomics was confirmed by flow cytometry (Figure 4B). Low expression of TLR4 in both Mϕ populations seen in the proteomics data was also confirmed by flow cytometry (Figure 4A, B).

Similarly, proteomic analysis showed clear enrichment of several Mϕ growth factor receptors (M-CSF-R (CSF1R) and GM-CSF-R (CSF2RA, B) in PM, whereas the transcript levels were similar for both PM and SRPM (Figure 4A). Expression levels of CSF1R, determined by flow cytometry, were in good agreement with the proteomic data (Figure 4A, B).

Similar observations were made with a number of other cell surface receptors (Figure 4C, D). While the proteomics and transcriptome data were consistent for expression levels of TIMD4, EMR1, CD163, CD206 and SIGLEC12, no correlation was seen for CD200R1, CD244, CD80, CD44, SIRP-A, CD86 and MS4A1. As above, the flow cytometry analysis was consistently in agreement with the proteomics data (Figure 4D).

Further proteomic analysis identified a wide variety of cell surface proteins (Figure 5 and Figure 6) that are important for Mϕ innate immune defence. These include galectins (LGALS1,3,8,9/ galectins 1, 3, 8, 9), Fc receptors (FCGR2, FCGRT, FCGR3, FCRL1, FCGR1, FCGR4, FCER1G), purinergic receptors (P2RX4, P2RX7), chemokine, cytokine and growth factor receptors (Figure 5 and Figure 6) that are expressed similarly by SRPM and PM (Figure 3–Figure 6). Although there was considerable overlap, these tissue Mϕs express a large set of differentially expressed membrane proteins involved in recognition and immune function. Figure 7 provides a pictorial overview and the copy number of these membrane proteins for each Mϕ population with fold enrichment greater than $\log_2 3$. In brief, for PM (Figure 7A), these include integrins and adhesion molecules (such as ITGAM, ITGA6, NINJ1, ICAM2, BCAM, ANTXR2/CAM, CEACAM1), lectins (CLEC10A, SELP, SELPLG, COLEC12), cytokine, chemokine receptors,

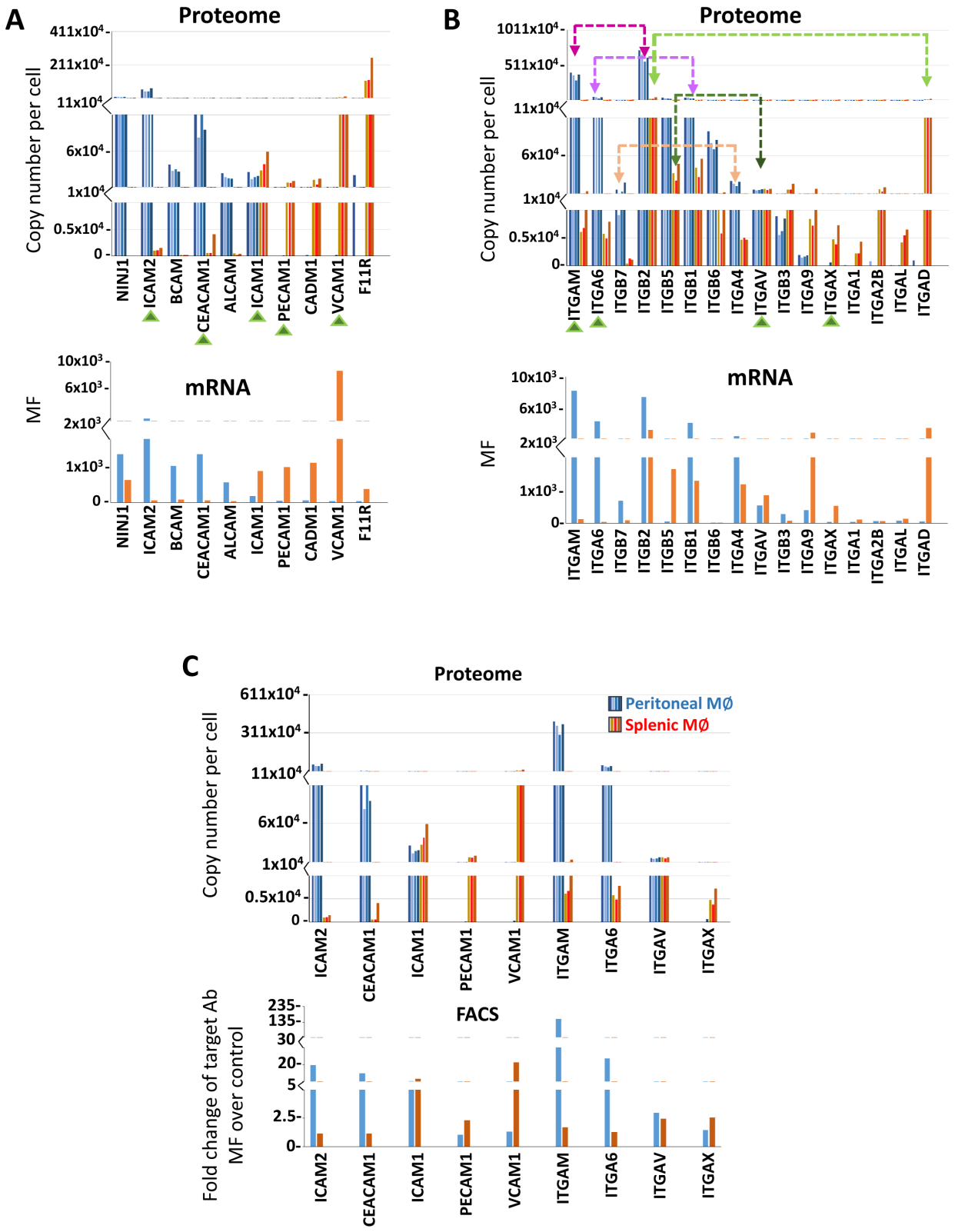

Figure 3. Expression levels of adhesion molecules based on proteomics, transcriptomics and flow cytometry. Cell adhesion molecules (**A**) and integrins (**B**), showing the estimated protein copy numbers per cell using the proteomic ruler approach (upper panels) and mean fluorescence of corresponding mRNA data obtained from the ImmGen database (lower panels). (**C**) Flow cytometry was used to validate proteomics for selected adhesion molecules. Upper panels show protein copy numbers per cell and lower panels show fold change in mean fluorescence values measured by flow cytometry, comparing specific antibodies with isotype matched controls.

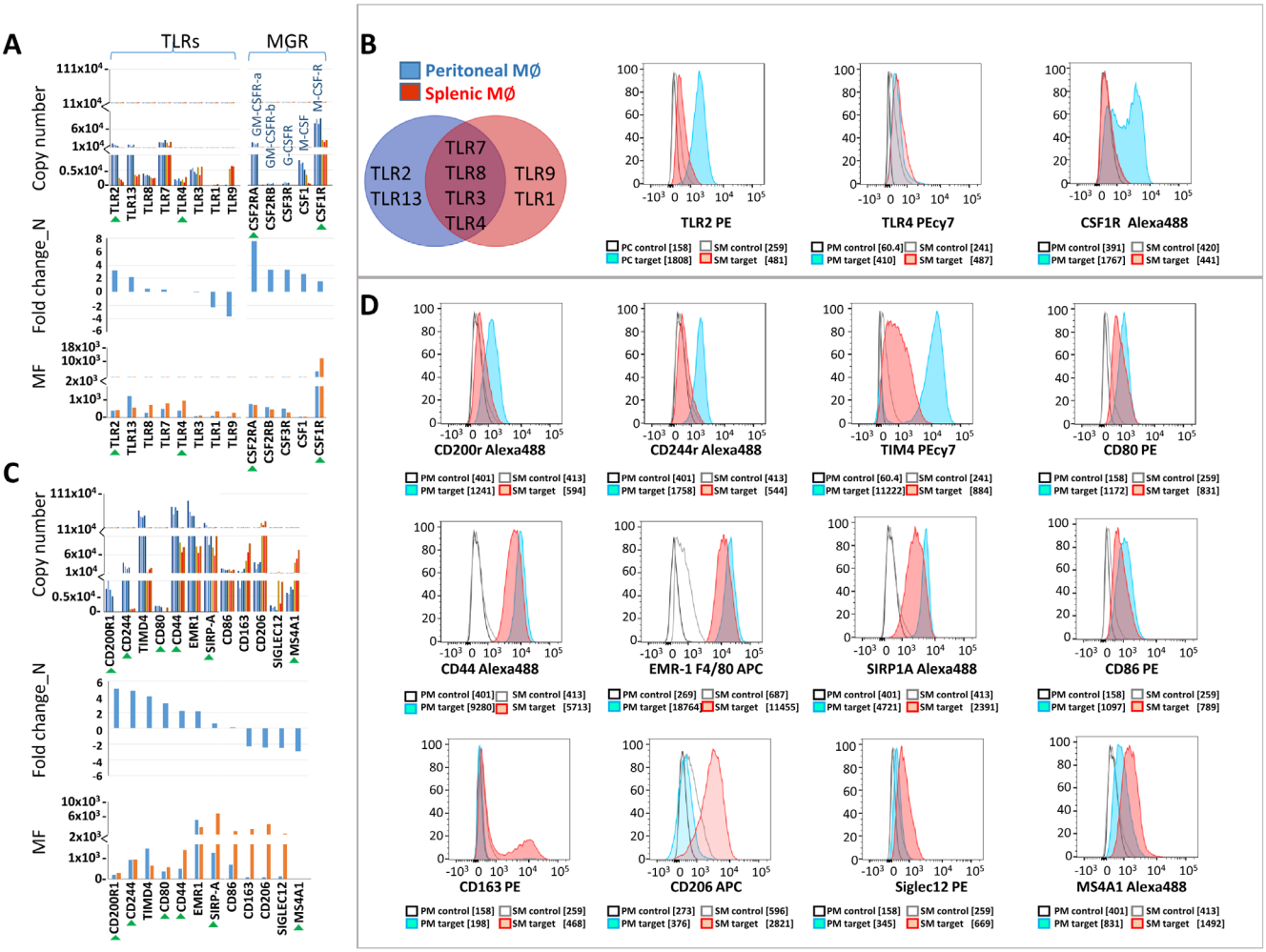

Figure 4. Expression levels obtained by proteomics is in concordance with cellular expression, even for gene IDs where proteomic data do not correlate with transcriptome. PM and SRPM expression of Toll-like receptors and growth factor receptors (**A**, **B**), cell surface immunoreceptors (**C**, **D**). (**A**, **C**) Estimated protein copy number per cell (upper panel), log fold protein increase in PM versus SRPM (middle panels) and mean fluorescence of mRNA expression (ImmGen) (lower panels). (**B**, **D**) Flow cytometry analysis for the indicated cell surface proteins. Green arrowheads in (**A**) and (**C**) show the gene IDs which are not in correlation between the proteome and the transcriptome and validated by flow cytometry. Chart in (**B**) shows distribution of TLR expression in PM and SRPM.

(CSF2RA, CRLF2, CCR, IFITM3), complement and coagulation factor receptors (C5AR1, CD93/C1QR, CD209B, PLAUR), Toll-like receptors (TLR2), scavenger receptors (MARCO, MSR1, CD36, STAB1, LYVE1) Purinergic receptor (P2RX1), immune-inhibitory receptors (VISTA, CD200R1, PILRA, PTGFRN), and number of other multifunctional receptors (MST1R, CD300LG, MCEMP1, GPM6A, FGFR1, EDNRB, SRA1). Likewise, for SRPM (Figure 7B), these include adhesion factors such as ITGAD, F11R, VCAM1, CADM1, PECAM1, C-type lectins (CLEC1B, CLEC4N;CLEC6A, CLEC4A, CLEC12A), sialic acid binding receptors (SIGLEC-1, SIGLEC-12/SIGLEC-E), lipid and peptide antigen presenting molecules (CD1D1, H2-AB1, H2-AA, H2-EB1, H2-OB, H2-M3), Toll-like receptors (TLR9), scavenger receptors (MRC1/CD206, CD68, CD163), a purinergic receptor (P2YR13), immune-inhibitory receptors (CD300A, CD300LF, CD274) and number of other multifunctional membrane proteins such as CYSTM1, AXL, CD82, MS4A1, CD79B, GFRA2, THY1, PDGFRB and REEP5.

Another key group of membrane proteins are the Slc and ABC families of transporters. These are essential for the import and export of many small molecules that are vital for regulation of metabolic processes and immune responses. Both PM and SRPM express a large number of these transporters in common, as shown in Figure 8. However, some are differentially expressed and enriched above $\log_2$3-fold. For PM, these include the ABC family transporter ABCA9 and Slc family transporters SLC2A6, SLC9A3R2, SLC25A15, SLC15A2, SLC16A3, SLC31A1, SLC25A1, SLC25A13 and SLC25A15. For SRPM, these include the ABC family transporter ABCG3 and Slc family

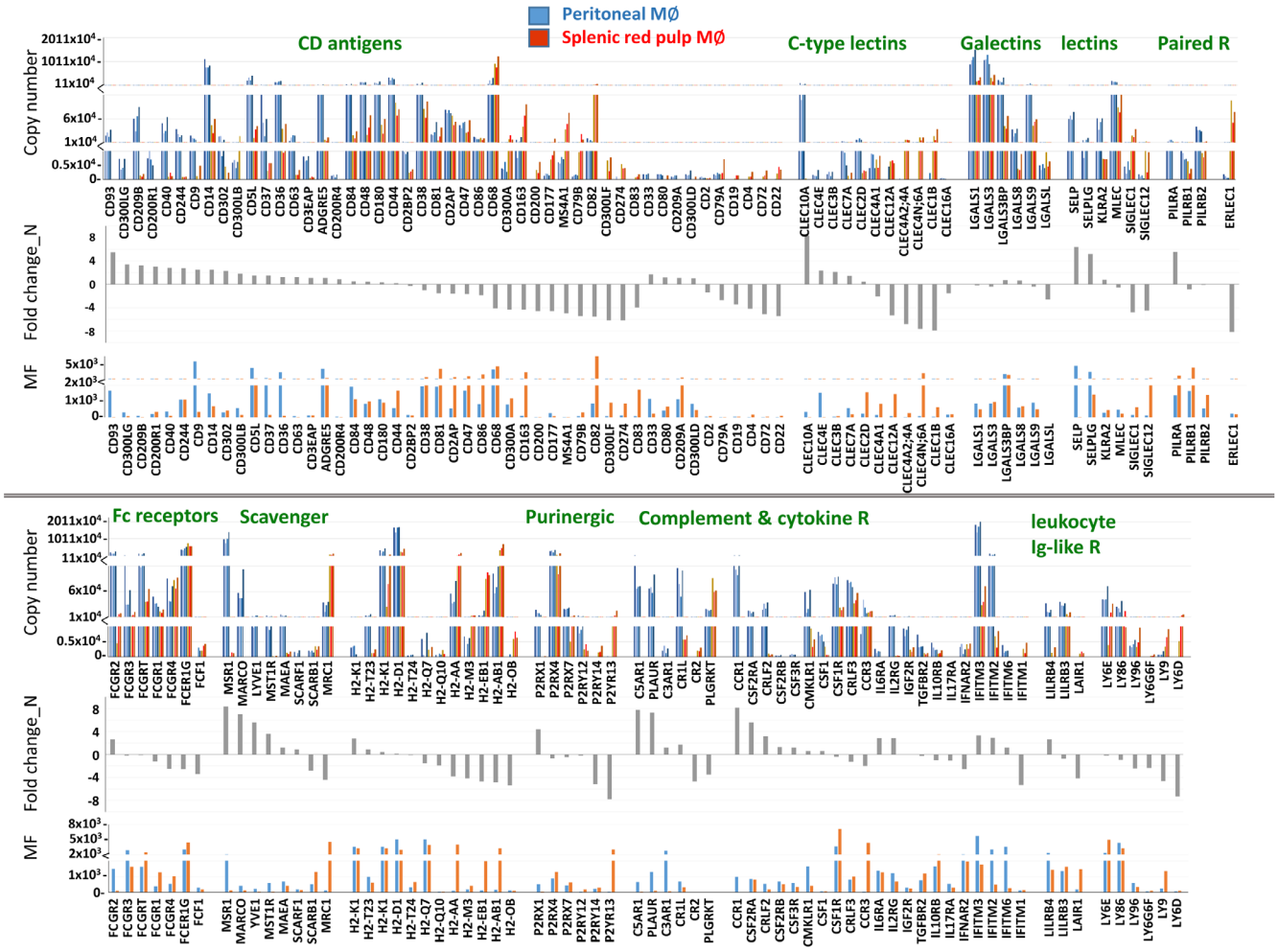

Figure 5. Characterization of CD markers and membrane receptors that are common and tissue specific. Graphs show the estimated protein copy numbers per cell using the proteomic ruler approach for proteome data set (upper panels), log fold protein increase in PM versus SRPM (middle panels) and mean fluorescence of mRNA data set obtained from ImmGen (lower panels).

transporters SLC3A2, SLC29A3, SLC35F6, SLC29A1, SLC12A2, SLC4A1, SLC37A2, SLC45A3 and SLC40A1;FPN1. Figure 6C provides a pictorial overview of their localisation and functions.

These findings indicate that, while the membrane proteins of PM and SRPM overlap considerably, a large set of membrane proteins is differentially expressed by these MΦs which are likely to contribute to their tissue-specific functions, as discussed in the next section.

Proteins important in known tissue-specific functions of peritoneal cavity and splenic red pulp macrophages

Although PM and SRPM have similar embryonic origins[33], they undergo tissue-specific differentiation programmes and mediate distinct functions within each microenvironment. This is clearly reflected in the proteomic data, as discussed below.

For PM, the transcription factor GATA6 was shown to be key regulator that defines a tissue-specific gene expression programme[34]. We observed enrichment of GATA6 as well as the reported GATA6-dependent PM-specific proteins such as SERPINB2, SELP (CD62P), THBS1, NT5E (CD73), TGFB2 and LTBP1 in our PM proteome (Figure 9A).

Vitamin A is required for induction of GATA6-dependent and -independent PM-specific gene expression programmes[34]. For vitamin A (retinol) to be transcriptionally active, it needs to be oxidized to the biologically active metabolite, retinoic acid (RA)[35–37]. Our proteomic analysis showed that RALDH2, the rate-limiting enzyme in RA synthesis[35,38], is highly expressed in PM. This suggests that PM may be capable of converting vitamin A to RA and that the omentum may not be required for this step as proposed by Okabe (Okabe 2014). Further, RA exerts its biological effects, primarily, through nuclear receptors RARs/RXRs and the non-nuclear receptor M6P/IGF2R[39–43]. In our proteome, we observed enhanced expression of RA receptors such as RXRB, RXRA, RARG and IGF2R in PM compared to SRPM (Figure 9A).

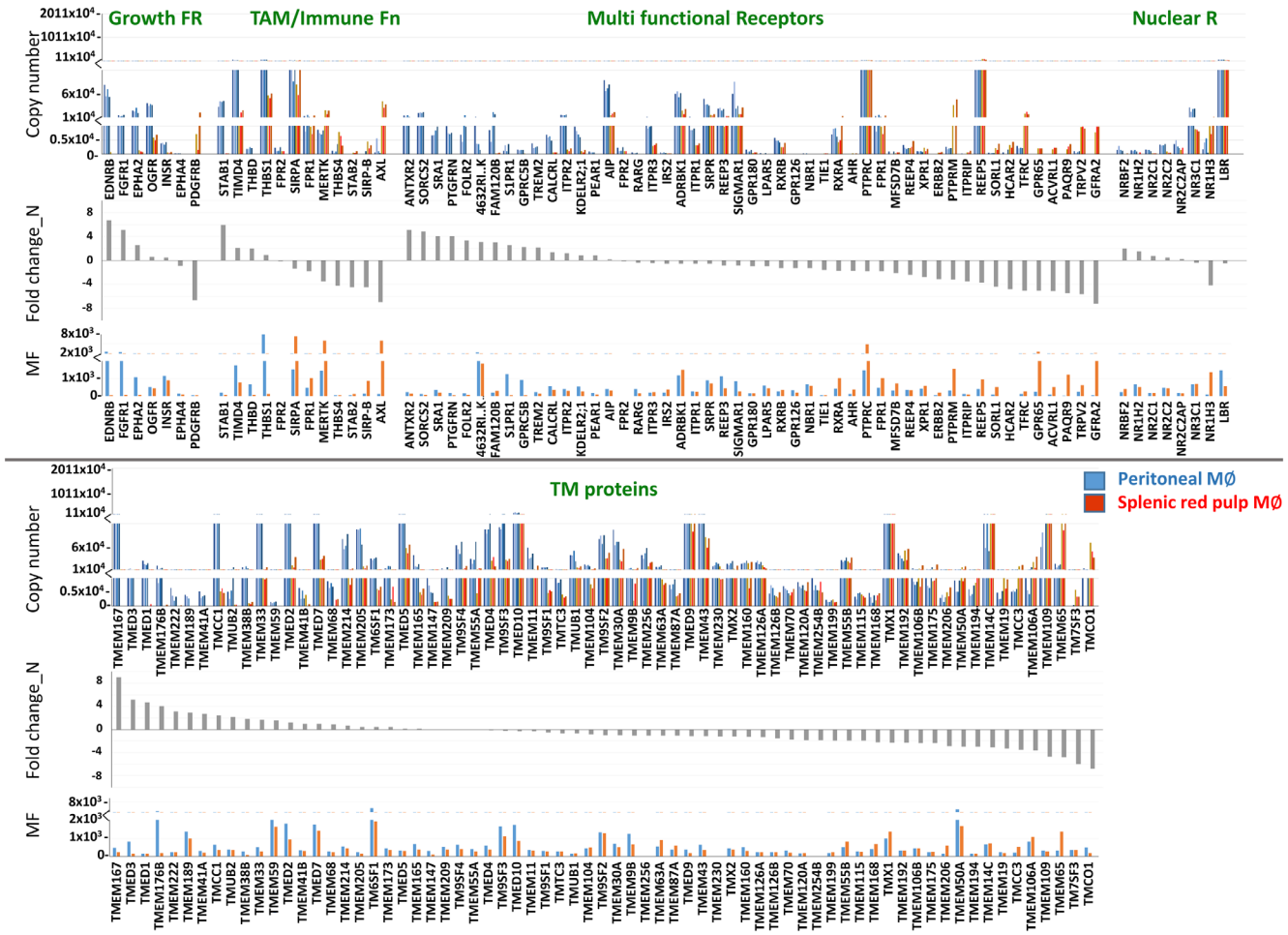

Figure 6. Characterization of membrane proteins that are common and tissue specific. Graphs show the estimated protein copy numbers per cell using the proteomic ruler approach for proteome data set (upper panels), log fold protein increase in PM versus SRPM (middle panels) and mean fluorescence of mRNA data set obtained from ImmGen (lower panels).

Furthermore, in the PM proteome we observed enrichment of proteins such as CXCL13, TGFB2 and CD44 that have been implicated in PM function (Figure 9A). CXCL13, is essential for B-1 cell (major peritoneal cavity B cell population) migration to the peritoneal cavity[44]. TGF-β generated by PM has been implicated in B-1 cell class switching and the generation of IgA[45]. In addition to enrichment of TGF-β, we also observed enhanced expression of TGF-β-associated proteins such as TGFBRAP1, TGFBI in the PM proteome (Figure 9A). CD44 has been shown to be important for the movement of PM to the liver in a sterile liver injury model to facilitate tissue repair by phagocytosing damaged tissue[14].

For SRPM, SPI-C is a key transcription factor required for their development following its induction by Mϕ exposure to heme[46] (Figure 9B). Major functions of SRPM are in capture and degradation of aged erythrocytes, repair of damaged or infected erythrocytes and iron homeostasis. Our proteomics data show enrichment of TAM receptors AXL, MERTK and STAB2 on SRPM (Figure 9B), which are likely to be important for recognition of aged or damaged erythrocytes via exposed phosphatidylserine, leading to erythro-phagocytosis[47]. We observed enrichment of heme oxygenase 1 (HOM-1) and ferroportin (SLC40A1) in SRPM (Figure 9B) which are required for heme metabolism and the release of free iron[7]. We also observed enrichment of CD163, which is a high affinity scavenger receptor for hemoglobin-haptoglobin complexes[48] (Figure 9B).

Splenic *hematopoietic* stem and progenitor cells (*HSPCs*) localize in the red pulp near the sinusoids in parafollicular areas[49,50]. VCAM1 is important for retaining HSPCs and in splenic myelopoiesis and was also enriched in the proteome of SRPM (Figure 9A).

Insights into metabolic functions of peritoneal cavity macrophages

An important conceptual advance in the field of Mϕ biology, emerging from recent studies, is that Mϕ polarisation is

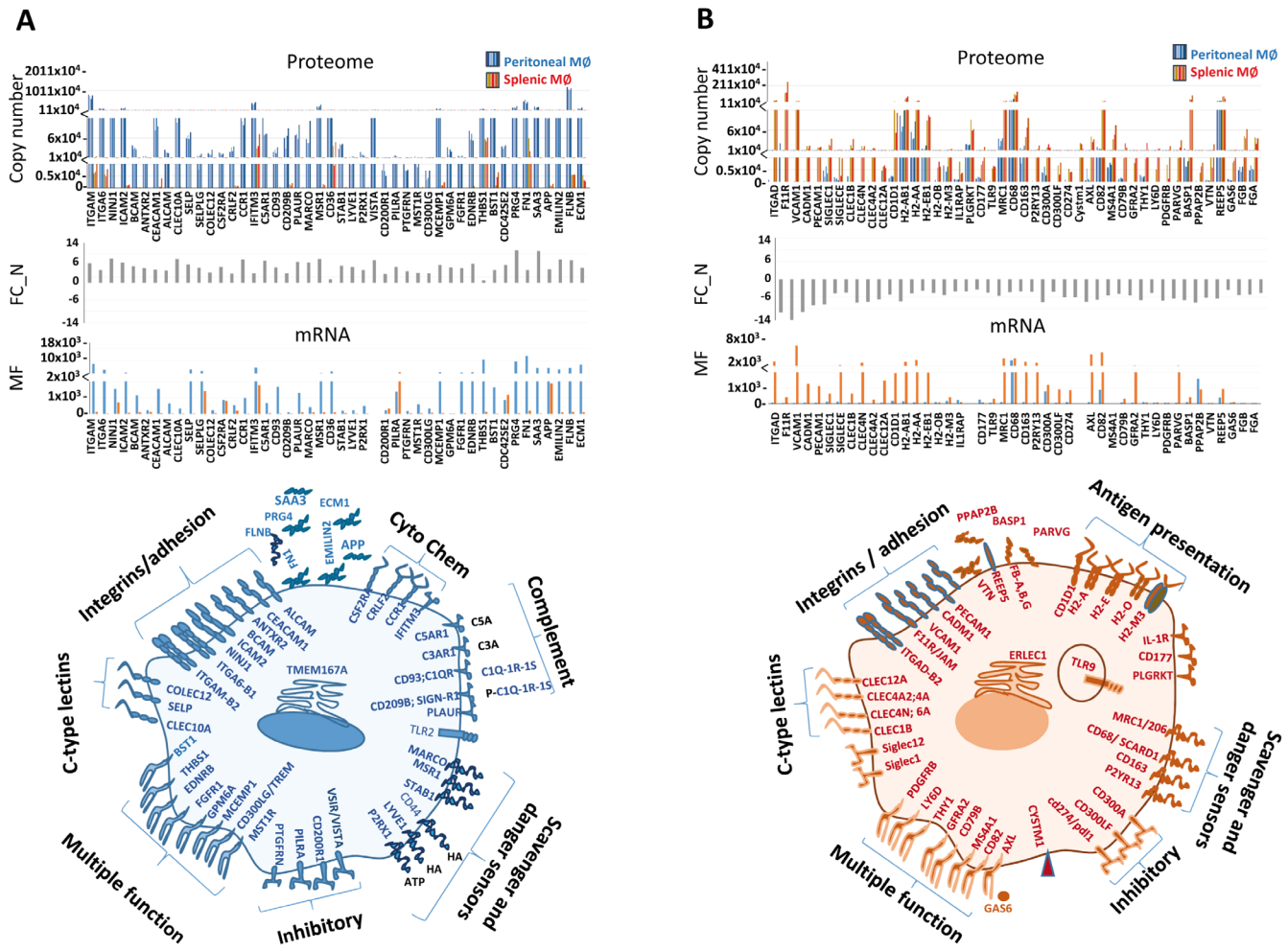

Figure 7. Characterization of CD markers and cell surface antigens that are tissue specific. Expression of surface proteins enriched in PM (**A**) and SRPM (**B**). Upper panels show the estimated protein copy numbers per cell, middle panels show log fold protein increase in PM versus SRPM and lower panels show mean fluorescence of mRNA expression (ImmGen). (**C**, **D**) Pictorial representation and functional categorisation of cell surface markers expressed on PM (**C**) or SRPM (**D**).

critically supported by metabolic shifts[51]. Therefore, in our proteomes we asked if any key metabolic enzymes are differentially regulated which could give insights into tissue-specific functions (Figure 10).

PM were enriched with enzymes related to glycolytic-citrate-lipogenic switch and generation of lipid secondary messengers. We observed enhanced expression of glucose transporter SLC2A6 (GLUT6/9) and key glycolytic enzymes (Figure 10A, B). These include HK1 (hexokinase-1), which traps glucose in the cell by converting it to glucose-6-phosphate; PFKL (ATP-dependent 6-phosphofructokinase liver type), the rate-limiting enzyme mediating the third step in glycolysis; KHK (ketohexokinase; fructokinase), the key enzyme for dietary fructose catabolism that bypasses the major glycolytic checkpoint (PFK) and converges into the glycolytic pathway. The enrichment of key glycolytic enzymes in PM suggests that these cells exhibit high rates of glycolysis (Figure 10A, B). Studies by others showed increased extracellular acidification rates (ECAR) in PM, which are indicators of glycolytic activity[52,53]. The enhanced expression of LDH (lactate dehydrogenase) and SLC16A3/MCT4 (Figure 8A), the lactate transporter[54], further supports the observed increase in ECAR and channelling of glycolysis towards lactate production in PM. Lactate at physiologic concentrations has been shown to play a role in visceral organ homeostasis, anti-inflammatory responses, wound healing and also acts as fuel donor through generation of pyruvate (via LDH)[55–60].

Furthermore, we noted that PM express high levels of ACLY (ATP citrate lyase), the enzyme responsible for generating cytosolic acetyl-CoA from citrate of the TCA cycle (Figure 10A, B). This suggests that pyruvate generated through glycolysis may be directed to alternate pathways other than TCA/OXPHOS, where citrate production is an end-product of glucose utilisation[61,62]. Supporting this hypothesis, previous

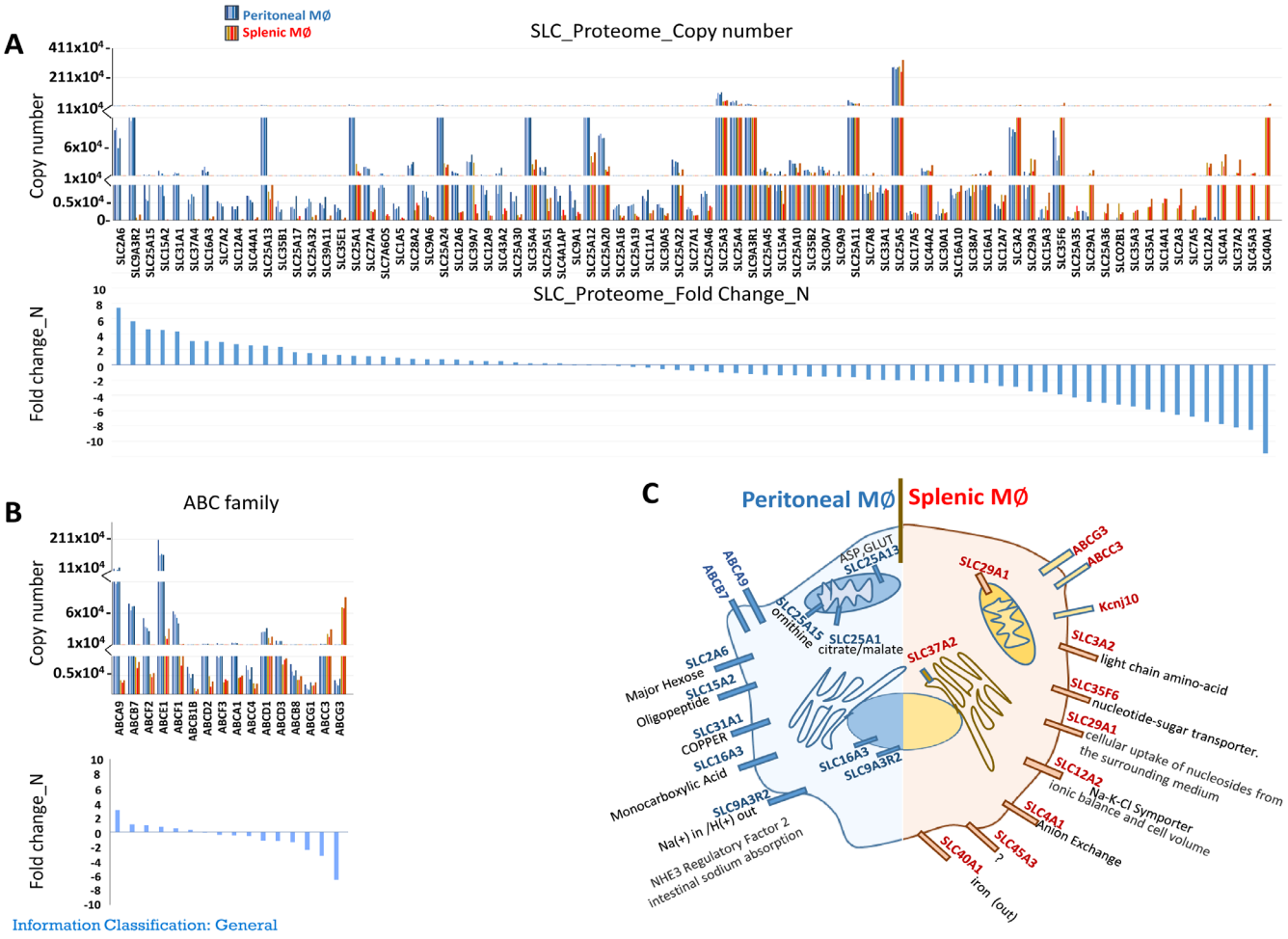

Figure 8. Characterization of SLC and ABC family transporters. Expression of SLC family transporters (**A**) and ABC family transporters (**B**) in PM and SRPM. Upper panels show the estimated protein copy numbers per cell, middle panels show log fold protein increase in PM versus SRPM and lower panels show log fold protein increase in PM versus SRPM. **C**: pictorial representation and functional categorisation of SLC and ABC family transporters on PM and SRPM.

studies with PM noted a marked difference in rates of CO_2 production from the 1st and 3rd carbon of pyruvate. It was noted that almost 60% of the [1-^{14}C] pyruvate that was utilized appeared as $^{14}CO_2$, whereas for the [3-^{14}C] pyruvate only about 15% of that utilized appeared as $^{14}CO_2$. This suggests a fate for acetyl-CoA produced from pyruvate other than OXPHOS[52,53,63]. Although these studies on CO_2 production were performed using thioglycollate-elicited PM, the ImmGen database showed high levels of ACLY (ATP citrate lyase) transcripts in both resident and thioglycollate-elicited PM.

ACLY is a key enzyme of *de novo* FA synthesis, as it generates cytosolic acetyl-CoA, an essential biosynthetic precursor for FA synthesis. In addition, the enhanced ASPA (aspartoacylase) levels in PM (Figure 10A, B) and availability of its substrate N-acetylaspartate in peritoneal fluid[52,64] could provide an additional source of acetyl donor for FA synthesis (Francis JS, 2016). Consistent with this idea, we observed enrichment of the rate-limiting enzyme of FA synthesis, ACACA (Acetyl-CoA Carboxylase Alpha), which converts cytosolic acetyl-CoA to malonyl CoA (Figure 10A and B). This pathway is important for M2 Mϕ development, as an inhibitor of acetyl-CoA carboxylase (ACACA) was shown to inhibit IL-4 induced M2 activation[65]. We also observed enrichment of ELOVL5 (fatty acid elongase 5), which catalyzes the rate-limiting reaction of the long-chain fatty acid (FA) elongation cycle and is vital in generation of mono/poly unsaturated FAs. Thus, the PM proteomics data show enrichment of key enzymes related to the glycolytic-citrate-lipogenic pathway. This is critical in many cells, including tumour cells, to fulfil bioenergetic and synthetic requirements[66]. In addition, we observed increased expression of FA-binding proteins FABP3, FABP4 and FABP7 which act as cytoplasmic lipid chaperones and are important in mediating metabolic balance and coordinating FA/lipid trafficking and lipid-mediated signalling in cells (Figure 10A and B).

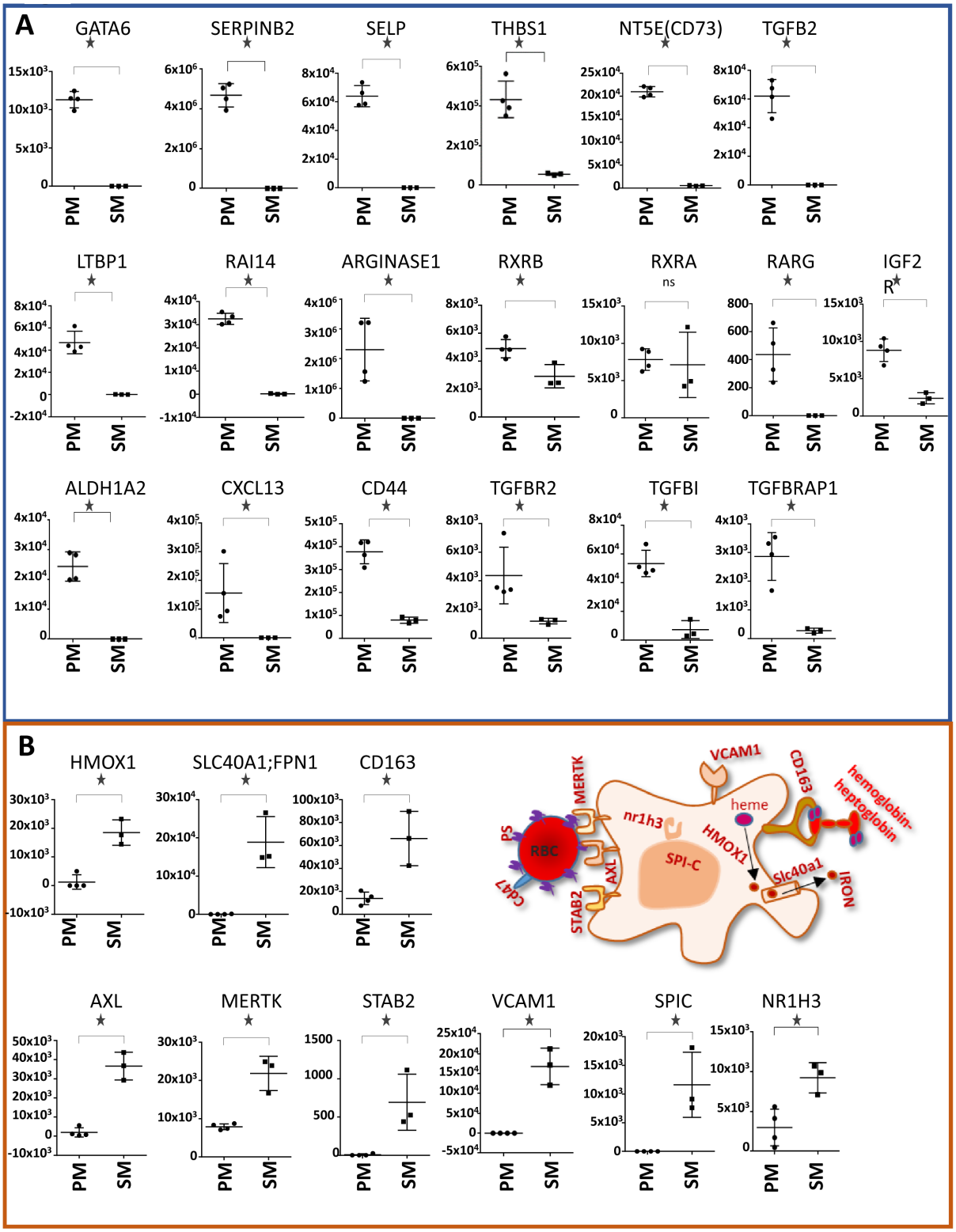

Figure 9. Enrichment of proteins related to tissue-specific functions. Peritoneal cavity specific functions (**A**) and spleen specific functions (**B**) showing protein copy numbers for PM and SRPM. Pictorial inset in (**B**) summarises SRPM protein functions. Statistical analyses were performed using Student's t-test. * indicates significant difference between peritoneal and SRPM ($p < 0.05$).

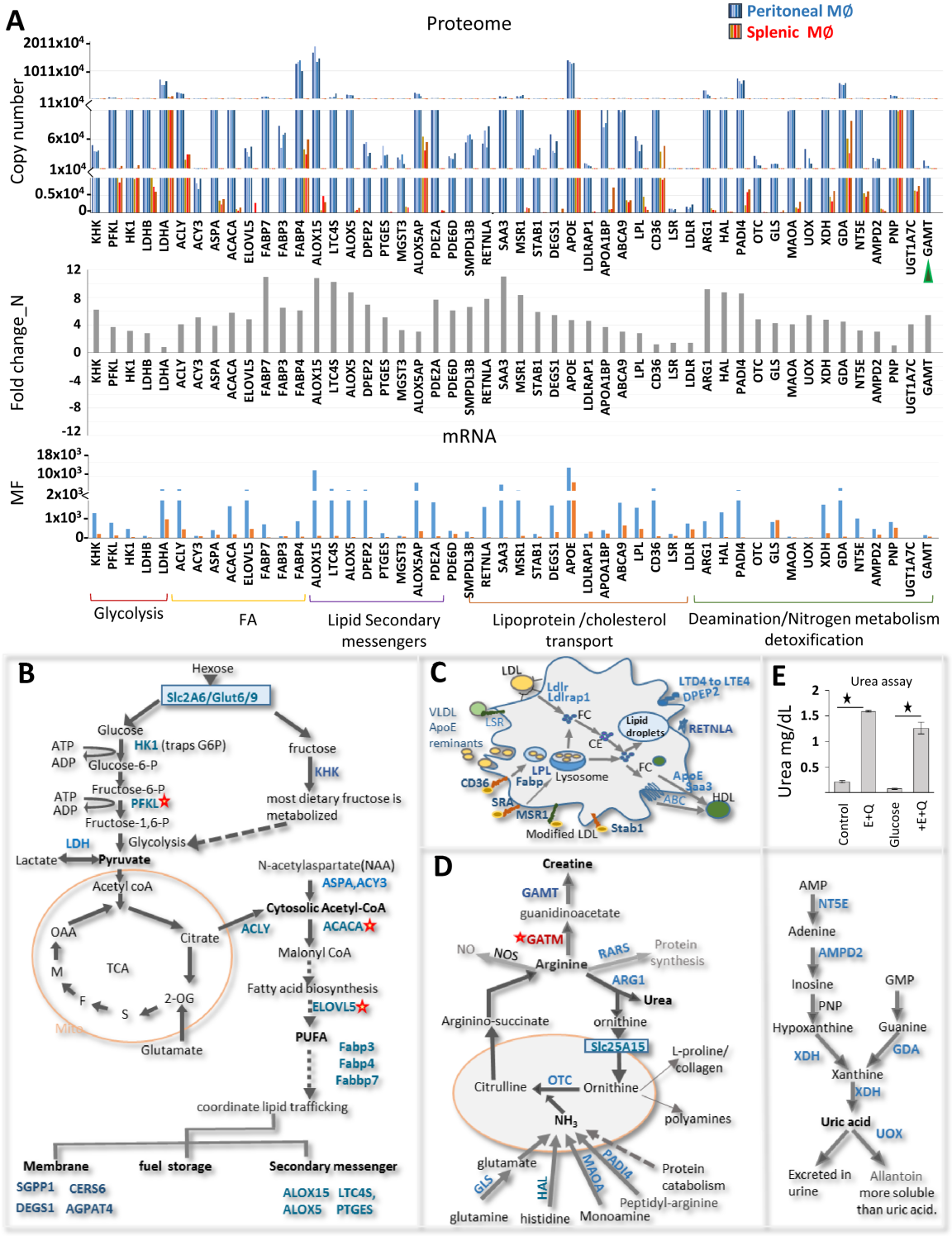

Figure 10. Metabolic pathway proteins enriched in peritoneal cavity macrophages. (**A**) Upper panel shows the estimated protein copy numbers per cell, middle panels show log fold protein increase in PM versus SRPM and lower panels show mean fluorescence of mRNA expression (ImmGen). (**B**) Pathway for glycolytic-lipogenic switch leading to generation of lipid messengers, as described in the Results section. (**C**) Pictorial representation showing LDL/VLDL uptake, catabolism and reverse cholesterol transport. (**D**) Gene IDs enriched in the pathways for detoxification and nitrogen homeostasis. Left panel shows the integration of deaminases into the urea cycle. Right panel shows pathways involved in purine catabolism. All the PM-enriched gene IDs are shown in blue. (**E**) Urea measurements in Mϕ culture supernatant after overnight incubation of PM with and without glutamine + glutamate. The first two bars are without glucose and the second two bars are with glucose. Red asterisks in (**B**) and (**D**) show the rate-limiting steps in the biosynthetic pathways.

FAs are essential for many aspects of cellular function. They not only act as a storage form of fuel, they are also important components of the cell membrane. When partially cleaved from the cell membrane, they form second messengers or local hormones such as arachidonic acid (AA) metabolites. These can mediate signalling in an autocrine or paracrine manner, thereby regulating inflammatory and immune responses and other vital cellular functions. Given that we observed enrichment in the PM proteome of key enzymes of FA synthesis (in particular Elovl5 that is required for the synthesis of monounsaturated and polyunsaturated FAs) as well as enrichment of many enzymes of the AA metabolic pathway (ALOX15, LTC4S, ALOX5, PTGR1, PTGES), this strongly suggests a role of FA synthesis in lipid secondary mediator generation (Figure 10A, B). Consistent with this idea, previous studies have observed that liver tissues of Elovl5-deficient mice had reduced levels of AA, eicosapentaenoic acid (EPA) and docosahexaenoic acid (DHA), which are precursors of the AA pathway mediators and substrates for ALOX15, LTC4S, ALOX5, PTGES[67,68]. Amongst these, ALOX15 (15-lipo-oxygenase) is the most abundant and is well documented for its role in resolution of inflammation via the generation of lipid mediators such as resolvins, protectins and maresins[14,69–71]. Given the fact that PM can be recruited to visceral organs and contribute to tissue repair[10–15], ALOX15 expression by PM may be important for resolution of inflammation, clearance of apoptotic cells and maintenance of tissue homeostasis, similar to findings made with Ly6C^{lo}, CX3CR1^{hi} Mϕs of liver and adipose tissue[69,71,72].

PM were enriched with enzymes related to lipoprotein uptake and cholesterol metabolism. Besides de novo synthesis, FAs can be acquired from extracellular sources via receptor-mediated uptake. The PM proteome exhibited increased levels of LDL/VLDL endocytic receptors, including CD36, MSR1, STAB1, LDLR, LSR. PM also expressed the lipoprotein lipase, LPL, which catalyses hydrolysis of triglycerides from LDL and VLDL (Figure 10A and C). Given that PM are relatively large and mobile cells, they may require contributions from both exogenous triacylglycerols and *de novo* synthesized FAs to meet increasing bioenergetics and demand for biosynthetic and lipid secondary metabolites, similar to that of M2 Mϕs[65].

We also observed enrichment of a number of proteins involved in regulation of cholesterol levels (Figure 10A, C), such as APOE (apolipoprotein E), RETNLA (adipokine resistin-like molecule alpha), SAA3 (serum amyloid A3) and ABCA9 (ATP-binding cassette family transporter)[73–76]. Gaudreault et al have shown that extra-hepatic sources of apoE produced by Mϕs play a role in lowering plasma cholesterol and providing protection against atherosclerosis[77]. The identification of several cholesterol regulating factors enriched in the PM proteome further supports this suggestion.

Interestingly, we observed that PM have elevated levels of enzymes related to nitrogen metabolism, detoxification, and immunoprotective function. Enzymes involved in catabolism of nitrogen-containing metabolites (amino acids, nucleotides and monoamines) and removal of toxic ammonia via the urea cycle were enriched in PM. These include ARG1 (arginase-1), GLS (glutaminase), HAL (histidase), MAOA (monoamine oxidase A), PADI4 (peptidylarginine deiminase type 4), GDA (guanine deaminase), AMPD2 (AMP deaminase 2), XDH (xanthine dehydrogenase) and UOX (urate oxidase) (Figure 10A, D). Among these, arginase-1 is the most studied enzyme in Mϕs. In PM it has been shown to play a role in the generation of urea[78] and in addition, we find that PM are able to utilise glutamine and glutamate which are rich in the peritoneum for urea generation (Figure 10E). This further supports the observation that fuel derived from glutaminolysis is exploited by PM to maintain the respiratory burst as suggested recently[52]. Arginase-1 is a key signature of alternatively activated Mϕs and is involved in a variety of immunomodulatory functions. By limiting the supply of L-arginine for NO synthase and by inhibiting inducible NO synthase activity via the generation of urea, arginase-1 mediates an anti-inflammatory function[78–80] (Figure 10D). Arginase-1 can also act extrinsically to suppress Th2 cytokine-driven inflammation via nutrient deprivation of L-arginine, which is required to sustain T cell responses[78]. Arginase-1 is also involved in the regulation of wound healing via synthesis of ornithine-proline-collagen[79,80].

Further, the proteomics data showed that XDH was strongly elevated in PM (Figure 10A, D). XDH, in addition to its role in purine catabolism (conversion of hypoxanthine/xanthine to uric acid), has been shown to play a significant role as a xenobiotic-detoxifier and also as a drug-metabolizing enzyme due to its relaxed specificity for substrates[81]. PM also expressed high levels of UGT1A7C (UDP-glucuronosyltransferase 1-7C) that catalyses glucuronidation, a major pathway of xenobiotic biotransformation in most mammalian species, that detoxifies many divergent chemical classes, rendering them harmless, more water-soluble, and hence excretable (Figure 10A). The proteomics therefore shows that PM are enriched with many proteins that play a significant role in nitrogen homeostasis and in detoxification of various endogenous and exogenous compounds.

Insights into immune functions of peritoneal cavity macrophages

Besides playing an important role in homeostasis, proteomics confirmed that PM are also well-equipped to perform important functions in immune defence. They expressed high levels of complement receptors (C5AR1, C3AR1, CD93; C1QR, CD209B; SIGN-R1)[82] and complement factors (C1R, CR1L, C1QB, C1QC, C1S, C4B, CFD, CFB, CFH) which provide a critical first-line defence against infection (Figure 11A). We also observed enrichment of various coagulation factors such as F5, F13A1, F10, F7, FN1, KNG1, PROS1, PLAUR, PLAU (Figure 11A)[83–85]. In particular, coagulation factor XIII (F13), which is highly enriched in PM, has been shown to take part in the early innate immune defence and significantly influences wound healing[85]. It limits bacterial dissemination and facilitates bacterial killing through their entrapment within fibrin networks[84]. In addition, a number of chemokines and immunomodulatory factors, as shown in Figure 11A, were enriched in PM that could play an important role in PM-mediated defence functions.

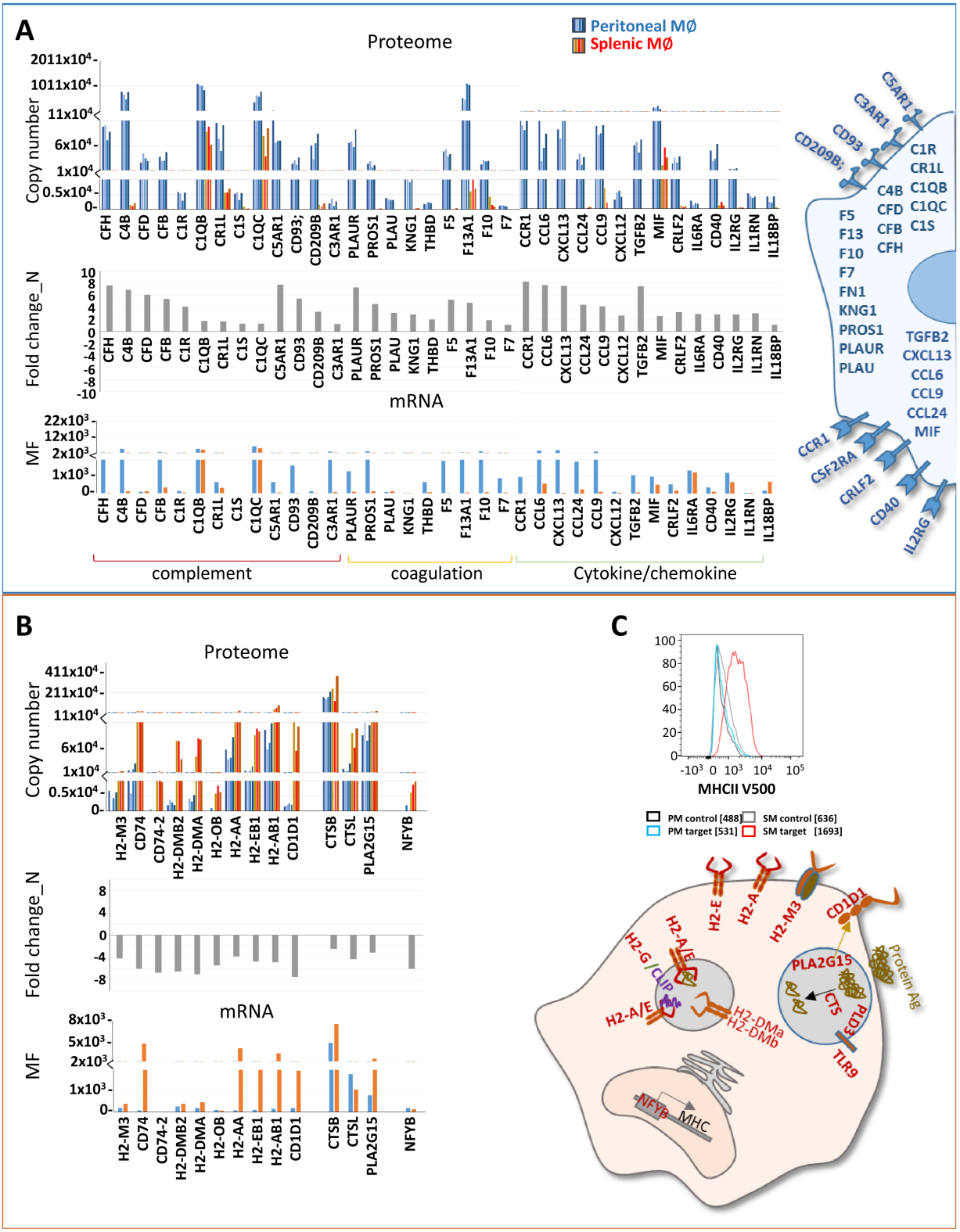

Figure 11. Immune defence proteins enriched in peritoneal cavity and splenic red pulp macrophages. (**A**) PM-enriched and (**B**) SRPM-enriched. Upper panels shows the estimated protein copy numbers per cell, middle panels show log fold protein increase in PM versus SRPM and lower panels show mean fluorescence of mRNA expression (ImmGen). (**C**) Expression of MHC-II on PM and SRPM analysed by flow cytometry (upper panel). Lower panel is a pictorial representation of SRPM gene IDs enriched in the pathway for peptide and lipid antigen presentation, as described in the *Results* section.

Insights into immune functions of splenic red pulp macrophages

For SRPM, in addition to enrichment of proteins involved in regulation of erythrocyte homeostasis, we observed enhanced expression of many proteins related to immune defence. Here we discuss some of the proteins that potentially play important functions in splenic tissue.

SRPM were enriched with proteins related to lipid and peptide antigen presentation. Antigen presentation via major histocompatibility complex class II molecules is highly critical in adaptive immunity. The processing and presentation of foreign proteins into small peptide fragments bound to class II molecules is a dynamic process consisting of multiple steps and chaperones. Several of the molecules involved in this process were enriched in SRPM compared to PM. We found enrichment of H2-A, H2-E (MHC-II) the class II antigen presenting molecules; H2-G (invariant chain (li/(CLIP)), the chaperone important in stabilising the peptide-binding groove of MHC-II/H2-DM that facilitates the exchange of the class II-associated invariant-chain peptide (CLIP) with peptides derived from exogenous antigens; CSTB and CSTL cathepsins, antigen-processing enzymes; the NFYB transcription factor that regulates MHC expression (Figure 11B). Flow cytometry analysis confirmed higher expression of MHC class II (H-2A and H-2E subclasses) molecules in SRPM compared to PM (Figure 11B).

We also observed enhanced expression of the non-classical class 1b histocompatibility antigen H2-M3 (Figure 11B). H2-M3 specifically bind to N-formylated peptides and is important in presenting *Listeria monocytogenes* and *Salmonella typhimurium* antigens to CTL[86,87].

Apart from factors involved in peptide antigen presentation, we also found preferential expression of lipid antigen presenting molecule, CD1D and PLA2G15 (lysosomal phospholipase A2) which processes lipid antigens for presentation by CD1d[88,89] (Figure 11B).

Thus, we observed enhanced expression of both lipid and foreign peptide presenting MHC-II molecules and their regulators in SRPM. In comparison, classical MHC class I molecules which present mainly endogenous peptides recognised by CD8+ (cytotoxic) T cells, were present at similar levels in the proteomes of SRPM and PM. In conclusion, the proteomics data suggest that SRPM may play a previously unrecognised role in regulation of adaptive immune responses, in addition to their homeostatic role in heme recycling and erythrocyte homeostasis.

SRPM were enriched in a number of defence proteins such as CTS (cathepsins), NGP (neutrophilic granule protein), MPO (myeloperoxidase), EPX (eosinophil peroxidase), EAR (eosinophil cationic protein), GZMA (granzyme A), ELANE (neutrophil elastase) and LTF (lactotransferrin) (Figure 12A). Many of these lytic mediators are associated with granulocytes but are also reported to be expressed by certain tissue Mϕs for pathogen defence[90–92]. Since SRPM have been shown to mediate efferocytosis of granulocytes in order to regulate steady-state granulopoiesis and HSPC trafficking[93–96], it is possible they acquired these factors through phagocytosis of apoptotic granulocytes[97,98]. This would also be consistent with low or undetectable mRNA encoding some of these proteins (Figure 12). However, other granulocyte markers like Gr-1(Ly6G/Ly6C) (neutrophils) and Siglec-F (eosinophils) were not detected (*Extended data*, Table 1)[18]. Finally, a number of immunomodulatory factors shown in Figure 12A, such as TGF-B1, IL1B, IL18, NOS1, IGF2, PPBP, CMC4 and serpin proteases, were enriched in SRPM. These could be important in host defence and clearance of foreign particles.

Insights into metabolic functions of splenic red pulp macrophages

SRPM were enriched with proteins related to glycan and lipid degradation enzymes. A major function of SRPM is the uptake of aged erythrocytes. This provides a significant phagocytic burden that has to be rapidly catabolised. We observed enhanced expression of endo-lysosomal glycan degradation enzymes such as ARSB (arylsulfatase B), IDS (iduronate 2-sulfatase), MANBA (beta-mannosidase), NPL (sialate lyase) (Figure 12B). Npl is a sialic acid degradation enzyme that prevents sialic acids from being recycled and returning to the cell surface. Given that sialic acid is an abundant sugar on erythrocytes, Npl and other glycan degradation enzymes are likely to be important for efficient catabolism of glycans on efferocytosed erythrocytes. We also noted enriched levels of endo-lysosomal lipases/exonucleases (Figure 12B) known to be involved in the clearance of efferocytosed particles[88,89,99–101]. These include PLBD1 (phospholipase B-like 1), ABHD6 (monoacylglycerol lipase), PLD3 (phospholipase D3) with both lipase and 5' exonucleases activities and PLA2G15 (lysosomal phospholipase A2) which plays a role in the processing and presentation of lipid antigens to CD1d. We also observed enrichment of LAP3 (cytosol aminopeptidase), ACP5 (acid phosphatase 5, lysosomal), a tartrate-resistant acid phosphatase, which catalyses the formation of ROS and participates in degradation of endocytosed bone matrix and in bacterial killing[102]. Key enzymes of beta oxidation were also enriched in SRPM such as ACSF2 (Acyl-CoA synthetase which is required to activate FA to enter beta oxidation) and ACADSB (mitochondrial acyl-CoA dehydrogenase) that initiates the first step of FA oxidation. The enhanced expression of this degradation machinery for glycans, proteins and lipids is likely to be important in the effective clearance of efferocytosed cells and foreign material by SRPM.

We identified several enzymes of lipid metabolism expressed preferentially in SRPM. These include phospholipases PLBD1, PLD3, HPGDS (hematopoietic PGD synthase) and HPGD (hydroxyprostaglandin dehydrogenase) (Figure 12B). HPGDS is the key enzyme for production of the D and J series of prostanoids in immune cells. PGD2 plays pro- or anti-inflammatory roles, where the outcome depends on the inflammatory milieu[103–107]. Though HPGDS and HPGD were found to be highly expressed in spleen, their tissue-specific functional significance is not well understood[108–111]. Also of note is the enrichment of

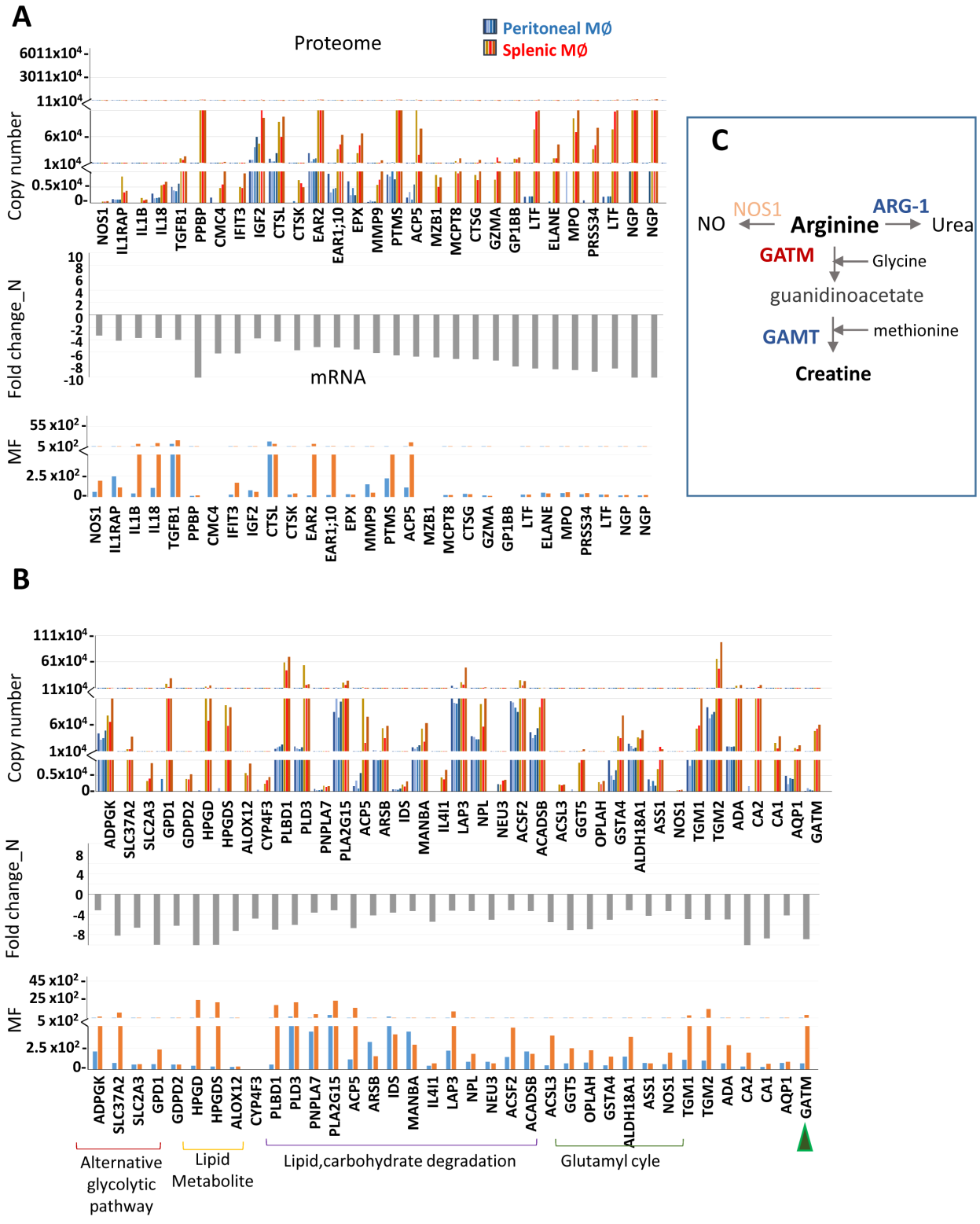

Figure 12. Immune defence and metabolic pathway proteins enriched in splenic red pulp macrophages. (**A**, **B**) Upper panels shows the estimated protein copy numbers per cell, middle panels show log fold protein increase in PM versus SRPM and lower panels show mean fluorescence of mRNA expression (ImmGen). Immune defence gene IDs (**A**) and metabolic pathway gene IDs (**B**) enriched in SRPM. (**C**), pictorial representation of differential nitrogen/arginine utilisation by PM and SRPM as discussed in the *Results* section. The PM gene IDs are in blue, SRPM in red.

GGT (gamma-glutamyltransferase), a membrane-bound enzyme involved in the metabolism of glutathione (gamma-glutamyl-cysteinyl-glycine; GSH) which can convert leukotriene C4 to leukotriene D4.

Other metabolic pathway enzymes that were enriched in SRPM with a potential role in immunomodulatory function are shown in Figure 12B with their absolute copy numbers, fold-change and mRNA levels. ADA (adenosine deaminase) was first identified in human spleen and is the predominant enzyme that converts the toxic DNA degradation product, deoxyadenosine to the non-toxic deoxyinosine. Elevated extracellular ADA activity has been observed in Mϕ-rich tissues, such as liver and spleen and shown to be important for acute and protracted inflammatory responses[112,113]. TGM1, TGM2 (transglutaminase) is a multi-functional enzyme that catalyses formation of isopeptide bonds between lysine and glutamine and produces protein-protein cross-links. In the context of immune defence, transglutaminases are required for migration of Mϕs towards apoptotic cells and for phagocytosis of apoptotic bodies. They also prevent the release of the pro-inflammatory cell content by crosslinking proteins of apoptotic cells and play both anti-inflammatory and inflammatory roles[114–116]. CA1 and CA2 (carbonic anhydrase 1, 2) are important enzymes involved in acid production. In osteoclasts, CA2 has been shown to be critically involved in demineralization of ectopic calcification, but with respect to SRPM, its function is unknown. Given that erythrocytes also express CA1 and CA2 and that we detected haemoglobin subunits in our proteome (Figure 12B and *Extended data,* Table 1)[18], it is possible that SRPM obtained some erythrocyte proteins via phagocytosis of aged erythrocytes[117–119]. This would also be consistent with low or undetectable mRNA encoding these proteins (Figure 12). However, retention of erythrocyte proteins appears to be selective, as other erythrocyte markers like glycophorins, erythrocyte membrane skeleton band protein band EPB4.2 and hemoglobin subunit-D[120] were low or undetectable (*Extended data,* Table 1)[18].

We observed enrichment in SRPM of non-canonical glycolytic pathway enzymes ADPGK (ADP-dependent glucokinase), GPD1 (glycerol-3-phosphate dehydrogenase), SLC2A3 (Glut3-glucose transporter) and SLC37A2 (G6PT) (Figure 12B). ADPGK catalyses noncanonical phosphorylation of glucose to glucose 6-phosphate using ADP as a phosphate donor and is highly expressed in human hematopoietic cells[121–123]. Studies with T-cells have shown that ADPGK activity resulted in a deviation of glycolysis towards the glycerol-3-phosphate dehydrogenase (GPD) shuttle, leading to increased mitochondrial ROS production. Given that we observed enrichment of, ADPGK, GPD1 and SLC2A3/GLUT3, a similar mechanism may be operational in SRPM[124] and contribute to their host defence functions. Furthermore, G6PT functions in glucose recycling between the ER and the cytoplasm and its deficiency leads to defective myeloid phenotypes, displaying impaired glucose homeostasis, neutropenia and neutrophil dysfunction[125–128]. Thus, we observed a number of proteins enriched in the SRPM proteome that could play roles in acute inflammation, pathogen defence and clearance (Figure 12B).

Creatine synthesis requires three amino acids, methionine, glycine, and arginine, and two enzymes, GATM (glycine amidinotransferase) and GAMT (guanidinoacetate N-methyltransferase). GATM is the rate limiting step in creatine synthesis, that catalyses the transfer of an amidino group from L-arginine to glycine to generate guanidinoacetate (GAA) and GAMT methylates guanidinoacetate (the immediate precursor of creatine) to produce creatine.

We observed elevated levels of GATM in the SRPM proteome and GAMT in the PM proteome (green arrowhead in Figure 10A, Figure 12B and 12C). Previous studies have shown the requirement of two organs for completion of creatine synthesis[129–131]. In the rat, high levels of GATM are found in the kidney, whereas GAMT is present in the liver. Rat hepatocytes were found to readily convert GAA to creatine; the same hepatocytes were unable to produce creatine from methionine, arginine, and glycine. ^{15}N from $^{15}NH_4Cl$ is readily incorporated into urea but not into creatine, suggesting the liver mainly utilises nitrogen in arginine for urea generation via the urea cycle and not for creatine synthesis[130,131]. Similar to hepatocytes, we found that PM have high levels of GAMT and not the first rate-limiting enzyme, GATM (last column, green arrowhead in Figure 10A, Figure 12B and 12C). Given that PM express high levels of arginine, they may channel the nitrogen in arginine for urea generation via the urea cycle and not for creatine synthesis, similar to the observations made with hepatocytes (Figure 12C). We hypothesise that, similar to the observations with kidney and liver, SRPM and PM may be coordinated for completion of creatine synthesis.

In general terms, SRPM appear to be functionally similar to a population of Mϕ recently described in human liver termed 'Non-inflammatory Macs -cluster 10' in single cell RNA-Seq data[132] and Kupffer cells of the mouse. All of these cells express high levels of VCAM1, SLC40A1, HMOX1, CD163, AXL, MERTK and play roles in the capture and breakdown of aged erythrocytes passing through the sinusoids[132–134]. In comparison, PM appear to share some of the functions of liver hepatocytes, with both cells expressing high levels of enzymes ARG1, HAL, GAMT, PFK-1, HK1 and SAA3 which play roles in metabolism of nitrogen-containing compounds, carbohydrates and lipids[78,132].

In conclusion, the present study provides a comprehensive view of the cellular profiling of Mϕs in different immune microenvironments and highlights the possible contributions of SRPM and PM populations in homeostasis and host defence that are adapted to each tissue environment.

Conclusions

This study has made effective use of a vast proteomic data set to obtain a better overall picture and understanding of the steady-state roles of splenic red pulp and peritoneal cavity Mϕs, defined mainly in terms of cell surface phenotype, metabolic pathways and immune functions (Figure 13). Given that several previous studies have demonstrated a low correlation between mRNA and protein expression, our proteomics analysis provides global profiling of these tissue Mϕs at a protein level, providing novel information on absolute copy number per cell. In addition,

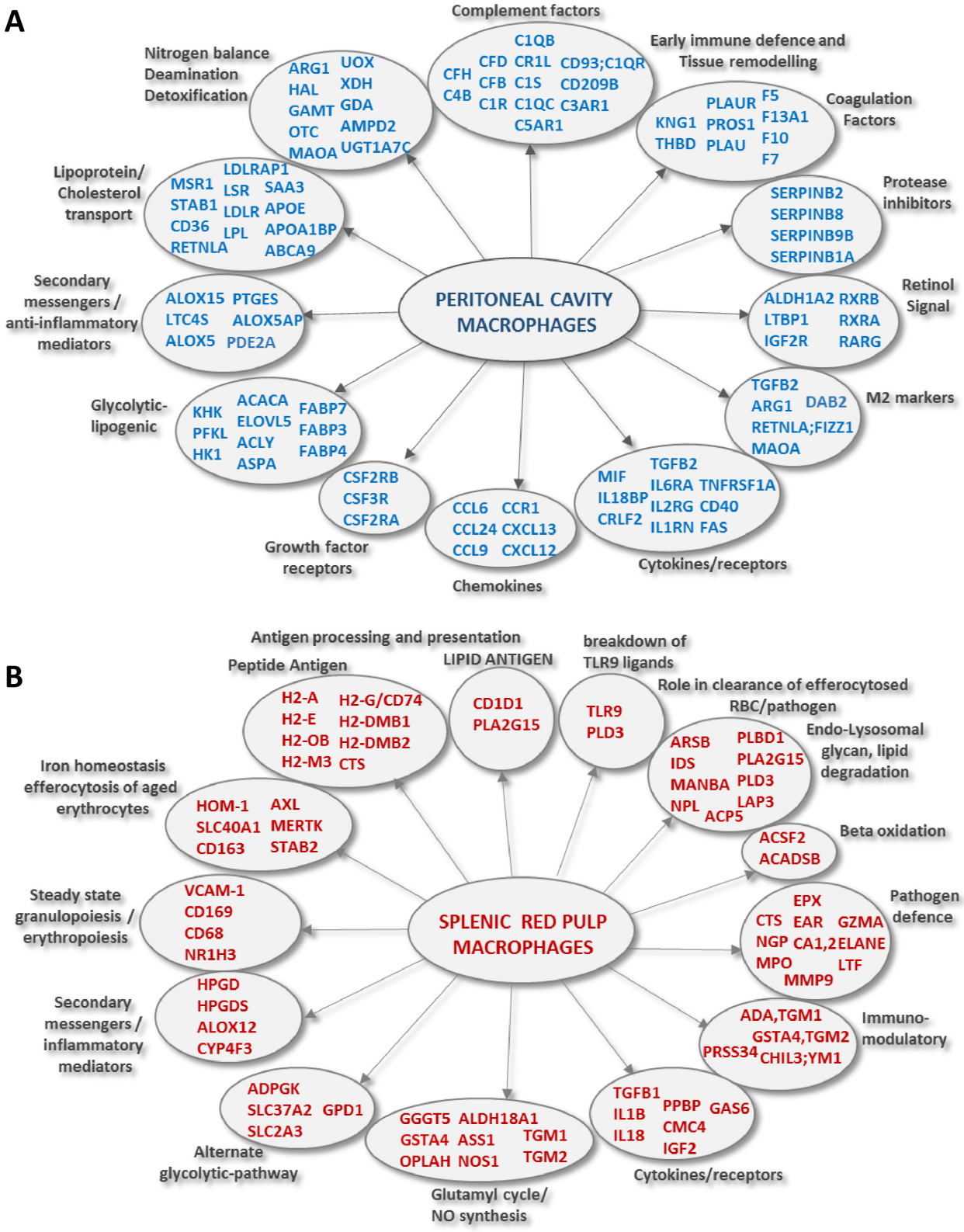

Figure 13. Pictorial representation of tissue specific pathways and functions enriched in PM (**A**) and SRPM (**B**), as discussed in the Results section.

the integration of our proteomics data sets with corresponding ImmGen transcriptomics data sets provides information on the relationships between the levels of transcripts and the proteins that they encode. This has not been examined previously in a comprehensive manner for tissue Mϕs. By merging these heterogeneous data sets we provide high-throughput data validation for the translation of mRNA to protein for many of the differentially expressed genes. We also show for the genes where mRNA and protein expression do not correlate, the cellular expression levels (as validated by flow cytometry) were in excellent agreement with the proteomics data. Thus, using quantitative proteomics, we have identified and validated several novel cellular differences between splenic and peritoneal Mϕs which were not addressed previously through transcriptomics studies.

We believe our characterization of cell surface markers, metabolic pathways and immune functions for PM and SRPM will be a useful resource in the Mϕ field. In particular, peritoneal Mϕs are easy to isolate and have therefore been used extensively as a model to study tissue Mϕ cell biology and immune functions. The availability of a comprehensive database of proteins expressed by these Mϕs and their relative abundance is important as it can help interpretations of complex results and provide guidance as to the suitability of these Mϕ for addressing specific scientific questions. Dissecting the cellular components and attempting to address why specific components are active at the cellular level using expression data and contextual information helps to understand their possible contribution to tissue specific functions. For example, many of the key enzymes that play roles in the catabolism of dietary fructose, carbohydrate and proteins and the removal of toxic ammonia (from excess amino acids and nitrogen catabolism) via the urea cycle, are enriched in peritoneal Mϕs. As predicted by these observations, we demonstrated that peritoneal Mϕs were able to effectively utilise glutamine and generate urea.

Thus, our approach, which builds upon connecting the mRNA expression data and protein networks, along with concepts proposed from previous publications of target genes, may pave the way to understanding the biological implications of the massive data available at both the mRNA and protein levels. In turn, this can give rise to novel hypotheses that can be tested experimentally.

Data availability

Underlying data

ProteomeXchange: Towards understanding tissue Mϕ heterogeneity and functions using quantitative proteomics. Accession number PXD019362; https://identifiers.org/px:PXD019362.

Mass spectrometry proteomics data are deposited with the ProteomeXchange Consortium via the PRIDE[135] partner repository.

Figshare: Towards understanding the cell surface phenotype, metabolic properties and immune functions of resident macrophages of the peritoneal cavity and splenic red pulp using high resolution quantitative proteomics. https://doi.org/10.6084/m9.figshare.c.5043488.v1[18].

This project contains the following underlying data:

- Data containing raw values for peptide quantification (XLSX) following FASP for use in MS.
- Data containing raw values for the urea assay (XLSX).
- The raw output values for FACS analysis (FCS) and the details of the experiments and linked files (PPT)

Extended data

Figshare: Towards understanding the cell surface phenotype, metabolic properties and immune functions of resident macrophages of the peritoneal cavity and splenic red pulp using high resolution quantitative proteomics. https://doi.org/10.6084/m9.figshare.c.5043488.v1[18].

This project contains the following extended data:

- **Table 1. Proteomics data set.** The table contains protein identifications and quantifications for peritoneal cavity Mϕ (PM) and splenic red pulp Mϕ (SM) obtained using proteomic analysis. The column headers describe the data in each column. The table also reports the copy number per cell for each experimental replicate obtained using the proteomic ruler quantifications and the relative fold change calculated using Perseus software as indicated in Methods.
- **Table 2. mRNA data set.** The table contains gene-expression profiles for peritoneal and splenic Mϕs obtained from the ImmGen dataset. The table contains mRNA profile data, their mean fluorescence intensities and the relative fold changes wherein affymetrix microarrays were used as the data collection platform. The column headers provide descriptions of the data contained within the table.
- **Table 3. Proteome and mRNA data sets combined.** The table contains protein quantification from the proteome dataset together with the corresponding transcripts from the ImmGen database which were used for the correlation analysis.
- **Table 4. Tissue-specific enriched proteins where proteome and mRNA data were positively correlated.** The table contains protein identifications where the correlation analysis showed 930 distinct transcripts with tissue-specific enrichment that were positively correlated with their corresponding proteins from the proteome data set.

Acknowledgments

We are grateful to the staff in our animal facility for their help in routine breeding and maintenance of mice. We would like to acknowledge the assistance of Abdel Atrih and others in the University of Dundee Proteomics Facility. We also thank the Flow Cytometry and Cell Sorting Facility at the University of Dundee for their assistance. Help from Iain Phair and Sarah Thomson with peritoneal Mϕ isolation in the initial stages of this project is gratefully acknowledged. This work benefitted from data assembled by the ImmGen consortium.

References

1. T'Jonck W, Guilliams M, Bonnardel J: **Niche signals and transcription factors involved in tissue-resident macrophage development.** *Cell Immunol.* 2018; **330**: 43–53.
PubMed Abstract | Publisher Full Text | Free Full Text

2. Haldar M, Murphy KM: **Origin, development, and homeostasis of tissue-resident macrophages.** *Immunol Rev.* 2014; **262**(1): 25–35.
PubMed Abstract | Publisher Full Text | Free Full Text

3. Zhou D, Yang K, Chen L, *et al.*: **Promising landscape for regulating macrophage polarization: epigenetic viewpoint.** *Oncotarget.* 2017; **8**(34): 57693–57706.
PubMed Abstract | Publisher Full Text | Free Full Text

4. Ivashkiv LB: **Epigenetic regulation of macrophage polarization and function.** *Trends Immunol.* 2013; **34**(5): 216–223.
PubMed Abstract | Publisher Full Text | Free Full Text

5. Wisniewski JR, Hein MY, Cox J, *et al.*: **A "proteomic ruler" for protein copy number and concentration estimation without spike-in standards.** *Mol Cell Proteomics.* 2014; **13**(12): 3497–3506.
PubMed Abstract | Publisher Full Text | Free Full Text

6. Zhang N, Czepielewski RS, Jarjour NN, *et al.*: **Expression of factor V by resident macrophages boosts host defense in the peritoneal cavity.** *J Exp Med.* 2019; **216**(6): 1291–1300.
PubMed Abstract | Publisher Full Text | Free Full Text

7. Kovtunovych G, Eckhaus MA, Ghosh MC, *et al.*: **Dysfunction of the heme recycling system in heme oxygenase 1-deficient mice: effects on macrophage viability and tissue iron distribution.** *Blood.* 2010; **116**(26): 6054–6062.
PubMed Abstract | Publisher Full Text | Free Full Text

8. Kohyama M, Ise W, Edelson BT, *et al.*: **Role for Spi-C in the development of red pulp macrophages and splenic iron homeostasis.** *Nature.* 2009; **457**(7227): 318–321.
PubMed Abstract | Publisher Full Text | Free Full Text

9. Klei TR, Meinderts SM, van den Berg TK, *et al.*: **From the Cradle to the Grave: The Role of Macrophages in Erythropoiesis and Erythrophagocytosis.** *Front Immunol.* 2017; **8**: 73.
PubMed Abstract | Publisher Full Text | Free Full Text

10. Cosin-Roger J, Ortiz-Masia D, Calatayud S, *et al.*: **The activation of Wnt signaling by a STAT6-dependent macrophage phenotype promotes mucosal repair in murine IBD.** *Mucosal Immunol.* 2016; **9**(4): 986–998.
PubMed Abstract | Publisher Full Text

11. Fraga-Silva TF, Venturini J, de Arruda MS: **Trafficking of phagocytic peritoneal cells in hypoinsulinemic-hyperglycemic mice with systemic candidiasis.** *BMC Infect Dis.* 2013; **13**: 147.
PubMed Abstract | Publisher Full Text | Free Full Text

12. Rehermann B: **Mature peritoneal macrophages take an avascular route into the injured liver and promote tissue repair.** *Hepatology.* 2017; **65**(1): 376–379.
PubMed Abstract | Publisher Full Text | Free Full Text

13. Song L, Papaioannou G, Zhao H, *et al.*: **The Vitamin D Receptor Regulates Tissue Resident Macrophage Response to Injury.** *Endocrinology.* 2016; **157**(10): 4066–4075.
PubMed Abstract | Publisher Full Text | Free Full Text

14. Wang J, Kubes P: **A Reservoir of Mature Cavity Macrophages that Can Rapidly Invade Visceral Organs to Affect Tissue Repair.** *Cell.* 2016; **165**(3): 668–678.
PubMed Abstract | Publisher Full Text

15. Zeng MY, Pham D, Bagaitkar J, *et al.*: **An efferocytosis-induced, IL-4-dependent macrophage-iNKT cell circuit suppresses sterile inflammation and is defective in murine CGD.** *Blood.* 2013; **121**(17): 3473–3483.
PubMed Abstract | Publisher Full Text | Free Full Text

16. Heng TS, Painter MW; Immunological Genome Project, C: **The Immunological Genome Project: networks of gene expression in immune cells.** *Nat Immunol.* 2008; **9**(10): 1091–1094.
PubMed Abstract | Publisher Full Text

17. Franken L, Klein M, Spasova M, *et al.*: **Splenic red pulp macrophages are intrinsically superparamagnetic and contaminate magnetic cell isolates.** *Sci Rep.* 2015; **5**: 12940.
PubMed Abstract | Publisher Full Text | Free Full Text

18. Nagala M: **Towards understanding the cell surface phenotype, metabolic properties and immune functions of resident macrophages of the peritoneal cavity and splenic red pulp using high resolution quantitative proteomics.** *Collection. Figshare.* 2020.
http://www.doi.org/10.6084/m9.figshare.c.5043488.v1

19. Wisniewski JR, Zougman A, Mann M: **Combination of FASP and StageTip-based fractionation allows in-depth analysis of the hippocampal membrane proteome.** *J Proteome Res.* 2009; **8**(12): 5674–5678.
PubMed Abstract | Publisher Full Text

20. Cox J, Mann M: **MaxQuant enables high peptide identification rates, individualized p.p.b.-range mass accuracies and proteome-wide protein quantification.** *Nat Biotechnol.* 2008; **26**(12): 1367–1372.
PubMed Abstract | Publisher Full Text

21. Cox J, Neuhauser N, Michalski A, *et al.*: **Andromeda: a peptide search engine integrated into the MaxQuant environment.** *J Proteome Res.* 2011; **10**(4): 1794–1805.
PubMed Abstract | Publisher Full Text

22. Tyanova S, Temu T, Cox J: **The MaxQuant computational platform for mass spectrometry-based shotgun proteomics.** *Nat Protoc.* 2016; **11**(12): 2301–2319.
PubMed Abstract | Publisher Full Text

23. Hofheinz K, Kakularam KR, Adel S, *et al.*: **Conversion of pro-inflammatory murine Alox5 into an anti-inflammatory 15S-lipoxygenating enzyme by multiple mutations of sequence determinants.** *Arch Biochem Biophys.* 2013; **530**(1): 40–47.
PubMed Abstract | Publisher Full Text

24. Wang C, Yu X, Cao Q, *et al.*: **Characterization of murine macrophages from bone marrow, spleen and peritoneum.** *BMC Immunol.* 2013; **14**: 6.
PubMed Abstract | Publisher Full Text | Free Full Text

25. Neeley ES, Kornblau SM, Coombes KR, *et al.*: **Variable slope normalization of reverse phase protein arrays.** *Bioinformatics.* 2009; **25**(11): 1384–1389.
PubMed Abstract | Publisher Full Text | Free Full Text

26. Vogel C, Marcotte EM: **Insights into the regulation of protein abundance from proteomic and transcriptomic analyses.** *Nat Rev Genet.* 2012; **13**(4): 227–232.
PubMed Abstract | Publisher Full Text | Free Full Text

27. Laurent JM, Vogel C, Kwon T, *et al.*: **Protein abundances are more conserved than mRNA abundances across diverse taxa.** *Proteomics.* 2010; **10**(23): 4209–4212.
PubMed Abstract | Publisher Full Text | Free Full Text

28. Waters KM, Pounds JG, Thrall BD: **Data merging for integrated microarray and proteomic analysis.** *Brief Funct Genomic Proteomic.* 2006; **5**(4): 261–272.
PubMed Abstract | Publisher Full Text

29. Piras V, Tomita M, Selvarajoo K: **Is central dogma a global property of cellular information flow?** *Front Physiol.* 2012; **3**: 439.
PubMed Abstract | Publisher Full Text | Free Full Text

30. Mathieson T, Franken H, Kosinski J, *et al.*: **Systematic analysis of protein turnover in primary cells.** *Nat Commun.* 2018; **9**(1): 689.
PubMed Abstract | Publisher Full Text | Free Full Text

31. Schwanhausser B, Busse D, Li N, *et al.*: **Global quantification of mammalian gene expression control.** *Nature.* 2011; **473**(7347): 337–342.
PubMed Abstract | Publisher Full Text

32. Ainslie MP, McNulty CA, Huynh T, *et al.*: **Characterisation of adhesion receptors mediating lymphocyte adhesion to bronchial endothelium provides evidence for a distinct lung homing pathway.** *Thorax.* 2002; **57**(12): 1054–1059.
PubMed Abstract | Publisher Full Text | Free Full Text

33. Varol C, Mildner A, Jung S: **Macrophages: development and tissue specialization.** *Annu Rev Immunol.* 2015; **33**: 643–675.
PubMed Abstract | Publisher Full Text

34. Okabe Y, Medzhitov R: **Tissue-specific signals control reversible program of localization and functional polarization of macrophages.** *Cell.* 2014; **157**(4): 832–844.
PubMed Abstract | Publisher Full Text | Free Full Text

35. Gudas LJ: **Emerging roles for retinoids in regeneration and differentiation in normal and disease states.** *Biochim Biophys Acta.* 2012; **1821**(1): 213–221.
PubMed Abstract | Publisher Full Text | Free Full Text

36. Kashyap V, Laursen KB, Brenet F, *et al.*: **RARgamma is essential for retinoic acid induced chromatin remodeling and transcriptional activation in embryonic stem cells.** *J Cell Sci.* 2013; **126**(Pt 4): 999–1008.
PubMed Abstract | Publisher Full Text | Free Full Text

37. Duester G: **Retinoic acid synthesis and signaling during early organogenesis.** *Cell.* 2008; **134**(6): 921–931.
PubMed Abstract | Publisher Full Text | Free Full Text

38. Blomhoff R, Green MH, Green JB, *et al.*: **Vitamin A metabolism: new perspectives on absorption, transport, and storage.** *Physiol Rev.* 1991; **71**(4): 951–990.
PubMed Abstract | Publisher Full Text

39. Kang JX, Li Y, Leaf A: **Mannose-6-phosphate/insulin-like growth factor-II receptor is a receptor for retinoic acid.** *Proc Natl Acad Sci U S A.* 1997; **94**(25): 13671–13676.
PubMed Abstract | Publisher Full Text | Free Full Text

40. Kang JX, Bell J, Leaf A, *et al.*: **Retinoic acid alters the intracellular trafficking of the mannose-6-phosphate/insulin-like growth factor II receptor and lysosomal enzymes.** *Proc Natl Acad Sci U S A.* 1998; **95**(23): 13687–13691.
PubMed Abstract | Publisher Full Text | Free Full Text

41. Rajawat Y, Hilioti Z, Bossis I: **Retinoic acid induces autophagosome maturation through redistribution of the cation-independent mannose-6-phosphate receptor.** *Antioxid Redox Signal.* 2011; **14**(11): 2165–2177.
PubMed Abstract | Publisher Full Text

42. Dolle P: **Developmental expression of retinoic acid receptors (RARs).** *Nucl Recept Signal.* 2009; **7**: e006.
PubMed Abstract | Publisher Full Text | Free Full Text

43. Spanjaard RA, Ikeda M, Lee PJ, *et al.*: **Specific activation of retinoic acid receptors (RARs) and retinoid X receptors reveals a unique role for RARgamma in induction of differentiation and apoptosis of S91 melanoma cells.** *J Biol Chem.* 1997; **272**(30): 18990–18999.
PubMed Abstract | Publisher Full Text

44. Ansel KM, Harris RB, Cyster JG: **CXCL13 is required for B1 cell homing, natural antibody production, and body cavity immunity.** *Immunity.* 2002; **16**(1): 67–76.
PubMed Abstract | Publisher Full Text

45. Roy B, Brennecke AM, Agarwal S, *et al.*: **An intrinsic propensity of murine peritoneal B1b cells to switch to IgA in presence of TGF-beta and retinoic acid.** *PLoS One.* 2013; **8**(12): e82121.
PubMed Abstract | Publisher Full Text | Free Full Text

46. Haldar M, Kohyama M, So AY, *et al.*: **Heme-mediated SPI-C induction promotes monocyte differentiation into iron-recycling macrophages.** *Cell.* 2014; **156**(6): 1223–1234.
PubMed Abstract | Publisher Full Text | Free Full Text

47. Chang CF, Goods BA, Askenase MH, *et al.*: **Erythrocyte efferocytosis modulates macrophages towards recovery after intracerebral hemorrhage.** *J Clin Invest.* 2018; **128**(2): 607–624.
PubMed Abstract | Publisher Full Text | Free Full Text

48. Estep TN: **Pharmacokinetics and mechanisms of plasma removal of hemoglobin-based oxygen carriers.** *Artif Cells Nanomed Biotechnol.* 2015; **43**(3): 203–215.
PubMed Abstract | Publisher Full Text

49. Dutta P, Hoyer FF, Grigoryeva LS, *et al.*: **Macrophages retain hematopoietic stem cells in the spleen via VCAM-1.** *J Exp Med.* 2015; **212**(4): 497–512.
PubMed Abstract | Publisher Full Text | Free Full Text

50. Kiel MJ, Yilmaz OH, Iwashita T, *et al.*: **SLAM family receptors distinguish hematopoietic stem and progenitor cells and reveal endothelial niches for stem cells.** *Cell.* 2005; **121**(7): 1109–1121.
PubMed Abstract | Publisher Full Text

51. Saha S, Shalova IN, Biswas SK: **Metabolic regulation of macrophage phenotype and function.** *Immunol Rev.* 2017; **280**(1): 102–111.
PubMed Abstract | Publisher Full Text

52. Davies LC, Rice CM, Palmieri EM, *et al.*: **Peritoneal tissue-resident macrophages are metabolically poised to engage microbes using tissue-niche fuels.** *Nat Commun.* 2017; **8**(1): 2074.
PubMed Abstract | Publisher Full Text | Free Full Text

53. Newsholme P, Gordon S, Newsholme EA: **Rates of utilization and fates of glucose, glutamine, pyruvate, fatty acids and ketone bodies by mouse macrophages.** *Biochem J.* 1987; **242**(3): 631–6.
PubMed Abstract | Publisher Full Text | Free Full Text

54. Dimmer KS, Friedrich B, Lang F, *et al.*: **The low-affinity monocarboxylate transporter MCT4 is adapted to the export of lactate in highly glycolytic cells.** *Biochem J.* 2000; **350 Pt 1**(Pt 1): 219–27.
PubMed Abstract | Free Full Text

55. Hoque R, Farooq A, Ghani A, *et al.*: **Lactate reduces liver and pancreatic injury in Toll-like receptor- and inflammasome-mediated inflammation via GPR81-mediated suppression of innate immunity.** *Gastroenterology.* 2014; **146**(7): 1763–74.
PubMed Abstract | Publisher Full Text | Free Full Text

56. Iraporda C, Errea A, Romanin DE, *et al.*: **Lactate and short chain fatty acids produced by microbial fermentation downregulate proinflammatory responses in intestinal epithelial cells and myeloid cells.** *Immunobiology.* 2015; **220**(10): 1161–9.
PubMed Abstract | Publisher Full Text

57. Lerch MM, Conwell DL, Mayerle J: **The anti-inflammasome effect of lactate and the lactate GPR81-receptor in pancreatic and liver inflammation.** *Gastroenterology.* 2014; **146**(7): 1602–5.
PubMed Abstract | Publisher Full Text

58. Nasi A, Fekete T, Krishnamurthy A, *et al.*: **Dendritic cell reprogramming by endogenously produced lactic acid.** *J Immunol.* 2013; **191**(6): 3090–9.
PubMed Abstract | Publisher Full Text

59. Peter K, Rehli M, Singer K, *et al.*: **Lactic acid delays the inflammatory response of human monocytes.** *Biochem Biophys Res Commun.* 2015; **457**(3): 412–8.
PubMed Abstract | Publisher Full Text

60. Sun S, Li H, Chen J, *et al.*: **Lactic Acid: No Longer an Inert and End-Product of Glycolysis.** *Physiology (Bethesda).* 2017; **32**(6): 453–463.
PubMed Abstract | Publisher Full Text

61. Costello LC, Franklin RB: **A review of the important central role of altered citrate metabolism during the process of stem cell differentiation.** *J Regen Med Tissue Eng.* 2013; **2**: 1.
PubMed Abstract | Publisher Full Text | Free Full Text

62. Williams NC, O'Neill LAJ: **A Role for the Krebs Cycle Intermediate Citrate in Metabolic Reprogramming in Innate Immunity and Inflammation.** *Front Immunol.* 2018; **9**: 141.
PubMed Abstract | Publisher Full Text | Free Full Text

63. Newsholme P, Newsholme EA: **Rates of utilization of glucose, glutamine and oleate and formation of end-products by mouse peritoneal macrophages in culture.** *Biochem J.* 1989; **261**(1): 211–218.
PubMed Abstract | Publisher Full Text | Free Full Text

64. Gautier EL, Ivanov S, Williams JW, *et al.*: **Gata6 regulates aspartoacylase expression in resident peritoneal macrophages and controls their survival.** *J Exp Med.* 2014; **211**(8): 1525–1531.
PubMed Abstract | Publisher Full Text | Free Full Text

65. Huang SC, Everts B, Ivanova Y, *et al.*: **Cell-intrinsic lysosomal lipolysis is essential for alternative activation of macrophages.** *Nat Immunol.* 2014; **15**(9): 846–855.
PubMed Abstract | Publisher Full Text | Free Full Text

66. Costello LC, Franklin RB: **'Why do tumour cells glycolyse?': from glycolysis through citrate to lipogenesis.** *Mol Cell Biochem.* 2005; **280**(1–2): 1–8.
PubMed Abstract | Publisher Full Text | Free Full Text

67. Moon YA, Hammer RE, Horton JD: **Deletion of ELOVL5 leads to fatty liver through activation of SREBP-1c in mice.** *J Lipid Res.* 2009; **50**(3): 412–423.
PubMed Abstract | Publisher Full Text | Free Full Text

68. Wang Y, Botolin D, Christian B, *et al.*: **Tissue-specific, nutritional, and developmental regulation of rat fatty acid elongases.** *J Lipid Res.* 2005; **46**(4): 706–715.
PubMed Abstract | Publisher Full Text | Free Full Text

69. Kwon HJ, Kim SN, Kim YA, *et al.*: **The contribution of arachidonate 15-lipoxygenase in tissue macrophages to adipose tissue remodeling.** *Cell Death Dis.* 2016; **7**(6): e2285.
PubMed Abstract | Publisher Full Text | Free Full Text

70. Tian R, Zuo X, Jaoude J, *et al.*: **ALOX15 as a suppressor of inflammation and cancer: Lost in the link.** *Prostaglandins Other Lipid Mediat.* 2017; **132**: 77–83.
PubMed Abstract | Publisher Full Text | Free Full Text

71. Uderhardt S, Herrmann M, Oskolkova OV, *et al.*: **12/15-lipoxygenase orchestrates the clearance of apoptotic cells and maintains immunologic tolerance.** *Immunity.* 2012; **36**(5): 834–846.
PubMed Abstract | Publisher Full Text

72. Yang W, Zhao X, Tao Y, *et al.*: **Proteomic analysis reveals a protective role of specific macrophage subsets in liver repair.** *Sci Rep.* 2019; **9**(1): 2953.
PubMed Abstract | Publisher Full Text | Free Full Text

73. Hayek T, Oiknine J, Brook JG, *et al.*: **Role of HDL apolipoprotein E in cellular cholesterol efflux: studies in apo E knockout transgenic mice.** *Biochem Biophys Res Commun.* 1994; **205**(2): 1072–1078.
PubMed Abstract | Publisher Full Text

74. Lee MR, Lim CJ, Lee YH, *et al.*: **The adipokine Retnla modulates cholesterol homeostasis in hyperlipidemic mice.** *Nat Commun.* 2014; **5**: 4410.
PubMed Abstract | Publisher Full Text

75. Mahley RW, Huang Y, Weisgraber KH: **Putting cholesterol in its place: apoE and reverse cholesterol transport.** *J Clin Invest.* 2006; **116**(5): 1226–1229.
PubMed Abstract | Publisher Full Text | Free Full Text

76. van der Westhuyzen DR, Cai L, de Beer MC, *et al.*: **Serum amyloid A promotes cholesterol efflux mediated by scavenger receptor B-I.** *J Biol Chem.* 2005; **280**(43): 35890–35895.
PubMed Abstract | Publisher Full Text

77. Gaudreault N, Kumar N, Olivas VR, *et al.*: **Macrophage-specific apoE gene repair reduces diet-induced hyperlipidemia and atherosclerosis in hypomorphic *Apoe* mice.** *PLoS One.* 2012; **7**(5): e35816.
PubMed Abstract | Publisher Full Text | Free Full Text

78. Pesce JT, Ramalingam TR, Mentink-Kane MM, *et al.*: **Arginase-1-expressing macrophages suppress Th2 cytokine-driven inflammation and fibrosis.** *PLoS Pathog.* 2009; **5**(4): e1000371.
PubMed Abstract | Publisher Full Text | Free Full Text

79. Durante W, Johnson FK, Johnson RA: **Arginase: a critical regulator of nitric oxide synthesis and vascular function.** *Clin Exp Pharmacol Physiol.* 2007; **34**(9): 906–911.
PubMed Abstract | Publisher Full Text | Free Full Text

80. Mills CD: **Macrophage arginine metabolism to ornithine/urea or nitric oxide/citrulline: a life or death issue.** *Crit Rev Immunol.* 2001; **21**(5): 399–425.
PubMed Abstract

81. Battelli MG, Polito L, Bortolotti M, *et al.*: **Xanthine Oxidoreductase in Drug**

Metabolism: Beyond a Role as a Detoxifying Enzyme. *Curr Med Chem.* 2016; **23**(35): 4027–4036.
PubMed Abstract | Publisher Full Text | Free Full Text

82. Kang YS, Do Y, Lee HK, *et al.*: **A dominant complement fixation pathway for pneumococcal polysaccharides initiated by SIGN-R1 interacting with C1q.** *Cell.* 2006; **125**(1): 47–58.
PubMed Abstract | Publisher Full Text

83. Inbal A, Dardik R: **Role of coagulation factor XIII (FXIII) in angiogenesis and tissue repair.** *Pathophysiol Haemost Thromb.* 2006; **35**(1–2): 162–165.
PubMed Abstract | Publisher Full Text

84. Loof TG, Morgelin M, Johansson L, *et al.*: **Coagulation, an ancestral serine protease cascade, exerts a novel function in early immune defense.** *Blood.* 2011; **118**(9): 2589–2598.
PubMed Abstract | Publisher Full Text

85. Soendergaard C, Kvist PH, Seidelin JB, *et al.*: **Tissue-regenerating functions of coagulation factor XIII.** *J Thromb Haemost.* 2013; **11**(5): 806–816.
PubMed Abstract | Publisher Full Text

86. Winther M, Holdfeldt A, Gabl M, *et al.*: **Formylated MHC Class Ib Binding Peptides Activate Both Human and Mouse Neutrophils Primarily through Formyl Peptide Receptor 1.** *PLoS One.* 2016; **11**(12): e0167529.
PubMed Abstract | Publisher Full Text | Free Full Text

87. Mir SA, Sharma S: **Role of MHC class Ib molecule, H2-M3 in host immunity against tuberculosis.** *Vaccine.* 2013; **31**(37): 3818–3825.
PubMed Abstract | Publisher Full Text

88. Paduraru C, Bezbradica JS, Kunte A, *et al.*: **Role for lysosomal phospholipase A2 in iNKT cell-mediated CD1d recognition.** *Proc Natl Acad Sci U S A.* 2013; **110**(13): 5097–5102.
PubMed Abstract | Publisher Full Text | Free Full Text

89. Shayman JA, Tesmer JJG: **Lysosomal phospholipase A2.** *Biochim Biophys Acta Mol Cell Biol Lipids.* 2018; **1864**(6): 932–940.
PubMed Abstract | Publisher Full Text | Free Full Text

90. Kulkarni NS, Hollins F, Sutcliffe A, *et al.*: **Eosinophil protein in airway macrophages: a novel biomarker of eosinophilic inflammation in patients with asthma.** *J Allergy Clin Immunol.* 2010; **126**(1): 61–69 e63.
PubMed Abstract | Publisher Full Text | Free Full Text

91. Dollery CM, Owen CA, Sukhova GK, *et al.*: **Neutrophil elastase in human atherosclerotic plaques: production by macrophages.** *Circulation.* 2003; **107**(22): 2829–2836.
PubMed Abstract | Publisher Full Text

92. Karakas M, Koenig W: **Myeloperoxidase production by macrophage and risk of atherosclerosis.** *Curr Atheroscler Rep.* 2012; **14**(3): 277–283.
PubMed Abstract | Publisher Full Text

93. Gordy C, Pua H, Sempowski GD, *et al.*: **Regulation of steady-state neutrophil homeostasis by macrophages.** *Blood.* 2011; **117**(2): 618–629.
PubMed Abstract | Publisher Full Text | Free Full Text

94. McCabe A, MacNamara KC: **Macrophages: Key regulators of steady-state and demand-adapted hematopoiesis.** *Exp Hematol.* 2016; **44**(4): 213–222.
PubMed Abstract | Publisher Full Text | Free Full Text

95. Furze RC, Rankin SM: **The role of the bone marrow in neutrophil clearance under homeostatic conditions in the mouse.** *FASEB J.* 2008; **22**(9): 3111–3119.
PubMed Abstract | Publisher Full Text | Free Full Text

96. Casanova-Acebes M, Pitaval C, Weiss LA, *et al.*: **Rhythmic modulation of the hematopoietic niche through neutrophil clearance.** *Cell.* 2013; **153**(5): 1025–1035.
PubMed Abstract | Publisher Full Text | Free Full Text

97. Gao CH, Dong HL, Tai L, *et al.*: **Lactoferrin-Containing Immunocomplexes Drive the Conversion of Human Macrophages from M2- into M1-like Phenotype.** *Front Immunol.* 2018; **9**: 37.
PubMed Abstract | Publisher Full Text | Free Full Text

98. Silva MT: **Macrophage phagocytosis of neutrophils at inflammatory/infectious foci: a cooperative mechanism in the control of infection and infectious inflammation.** *J Leukoc Biol.* 2011; **89**(5): 675–683.
PubMed Abstract | Publisher Full Text

99. Schneider BE, Behrends J, Hagens K, *et al.*: **Lysosomal phospholipase A2: a novel player in host immunity to *Mycobacterium tuberculosis*.** *Eur J Immunol.* 2014; **44**(8): 2394–2404.
PubMed Abstract | Publisher Full Text

100. Pribasig MA, Mrak I, Grabner GF, *et al.*: **alpha/beta Hydrolase Domain-containing 6 (ABHD6) Degrades the Late Endosomal/Lysosomal Lipid Bis(monoacylglycero)phosphate.** *J Biol Chem.* 2015; **290**(50): 29869–29881.
PubMed Abstract | Publisher Full Text | Free Full Text

101. Gavin AL, Huang D, Huber C, *et al.*: **PLD3 and PLD4 are single-stranded acid exonucleases that regulate endosomal nucleic-acid sensing.** *Nat Immunol.* 2018; **19**(9): 942–953.
PubMed Abstract | Publisher Full Text | Free Full Text

102. Raisanen SR, Alatalo SL, Ylipahkala H, *et al.*: **Macrophages overexpressing tartrate-resistant acid phosphatase show altered profile of free radical production and enhanced capacity of bacterial killing.** *Biochem Biophys Res Commun.* 2005; **331**(1): 120–6.
PubMed Abstract | Publisher Full Text

103. Trivedi SG, Newson J, Rajakariar R, *et al.*: **Essential role for hematopoietic prostaglandin D2 synthase in the control of delayed type hypersensitivity.** *Proc Natl Acad Sci U S A.* 2006; **103**(13): 5179–84.
PubMed Abstract | Publisher Full Text | Free Full Text

104. Kanaoka Y, Fujimori K, Kikuno R, *et al.*: **Structure and chromosomal localization of human and mouse genes for hematopoietic prostaglandin D synthase. Conservation of the ancestral genomic structure of sigma-class glutathione S-transferase.** *Eur J Biochem.* 2000; **267**(11): 3315–22.
PubMed Abstract | Publisher Full Text

105. Tanaka K, Ogawa K, Sugamura K, *et al.*: **Cutting edge: differential production of prostaglandin D2 by human helper T cell subsets.** *J Immunol.* 2000; **164**(5): 2277–80.
PubMed Abstract | Publisher Full Text

106. Mohri I, Taniike M, Taniguchi H, *et al.*: **Prostaglandin D2-mediated microglia/astrocyte interaction enhances astrogliosis and demyelination in twitcher.** *J Neurosci.* 2006; **26**(16): 4383–93.
PubMed Abstract | Publisher Full Text | Free Full Text

107. Mohri I, Eguchi N, Suzuki K, *et al.*: **Hematopoietic prostaglandin D synthase is expressed in microglia in the developing postnatal mouse brain.** *Glia.* 2003; **42**(3): 263–74.
PubMed Abstract | Publisher Full Text

108. Joo M, Sadikot RT: **PGD synthase and PGD2 in immune resposne.** *Mediators Inflamm.* 2012; **2012**: 503128.
PubMed Abstract | Publisher Full Text | Free Full Text

109. Kanaoka Y, Ago H, Inagaki E, *et al.*: **Cloning and crystal structure of hematopoietic prostaglandin D synthase.** *Cell.* 1997; **90**(6): 1085–95.
PubMed Abstract | Publisher Full Text

110. Meyer DJ, Thomas M: **Characterization of rat spleen prostaglandin H D-isomerase as a sigma-class GSH transferase.** *Biochem J.* 1995; **311**(Pt 3): 739–42.
PubMed Abstract | Publisher Full Text | Free Full Text

111. Urade Y, Fujimoto N, Ujihara M, *et al.*: **Biochemical and immunological characterization of rat spleen prostaglandin D synthetase.** *J Biol Chem.* 1987; **262**(8): 3820–3825.
PubMed Abstract

112. Chen W, Zhang S, Zhang W, *et al.*: **Elevated serum adenosine deaminase levels in secondary hemophagocytic lymphohistiocytosis.** *Int J Lab Hematol.* 2015; **37**(4): 544–550.
PubMed Abstract | Publisher Full Text

113. Apasov SG, Blackburn MR, Kellems RE, *et al.*: **Adenosine deaminase deficiency increases thymic apoptosis and causes defective T cell receptor signaling.** *J Clin Invest.* 2001; **108**(1): 131–141.
PubMed Abstract | Publisher Full Text | Free Full Text

114. Toth B, Garabuczi E, Sarang Z, *et al.*: **Transglutaminase 2 is needed for the formation of an efficient phagocyte portal in macrophages engulfing apoptotic cells.** *J Immunol.* 2009; **182**(4): 2084–2092.
PubMed Abstract | Publisher Full Text

115. Sarang Z, Madi A, Koy C, *et al.*: **Tissue transglutaminase (TG2) facilitates phosphatidylserine exposure and calpain activity in calcium-induced death of erythrocytes.** *Cell Death Differ.* 2007; **14**(10): 1842–1844.
PubMed Abstract | Publisher Full Text | Free Full Text

116. Szondy Z, Korponay-Szabo I, Kiraly R, *et al.*: **Transglutaminase 2 in human diseases.** *Biomedicine (Taipei).* 2017; **7**(3): 15.
PubMed Abstract | Publisher Full Text | Free Full Text

117. Barinda AJ, Ikeda K, Hirata KI, *et al.*: **Macrophages Highly Express Carbonic Anhydrase 2 and Play a Significant Role in Demineralization of the Ectopic Calcification.** *Kobe J Med Sci.* 2017; **63**(2): E45–E50.
PubMed Abstract | Free Full Text

118. Karhukorpi EK: **Carbonic anhydrase II in rat acid secreting cells: comparison of osteoclasts with gastric parietal cells and kidney intercalated cells.** *Acta Histochem.* 1991; **90**(1): 11–20.
PubMed Abstract | Publisher Full Text

119. Sundquist KT, Leppilampi M, Jarvelin K, *et al.*: **Carbonic anhydrase isoenzymes in isolated rat peripheral monocytes, tissue macrophages, and osteoclasts.** *Bone.* 1987; **8**(1): 33–38.
PubMed Abstract | Publisher Full Text

120. Bryk AH, Wisniewski JR: **Quantitative Analysis of Human Red Blood Cell Proteome.** *J Proteome Res.* 2017; **16**(8): 2752–2761.
PubMed Abstract | Publisher Full Text

121. Grudnik P, Kaminski MM, Rembacz KP, *et al.*: **Structural basis for ADP-dependent glucokinase inhibition by 8-bromo-substituted adenosine nucleotide.** *J Biol Chem.* 2018; **293**(28): 11088–11099.
PubMed Abstract | Publisher Full Text | Free Full Text

122. Hruz T, Laule O, Szabo G, *et al.*: **Genevestigator v3: a reference expression database for the meta-analysis of transcriptomes.** *Adv Bioinformatics.* 2008; **2008**: 420747.
PubMed Abstract | Publisher Full Text | Free Full Text

123. Wu C, Orozco C, Boyer J, *et al.*: **BioGPS: an extensible and customizable portal for querying and organizing gene annotation resources.** *Genome Biol.* 2009; **10**(11): R130.
PubMed Abstract | Publisher Full Text | Free Full Text

124. Kaminski MM, Sauer SW, Kaminski M, *et al.*: **T cell activation is driven by an ADP-dependent glucokinase linking enhanced glycolysis with mitochondrial reactive oxygen species generation.** *Cell Rep.* 2012; **2**(5): 1300–1315.
PubMed Abstract | Publisher Full Text

125. Chou JY, Mansfield BC: **The SLC37 family of sugar-phosphate/phosphate exchangers.** *Curr Top Membr.* 2014; **73**: 357–382.
PubMed Abstract | Publisher Full Text | Free Full Text

126. Cappello AR, Curcio R, Lappano R, *et al.*: **The Physiopathological Role of the Exchangers Belonging to the SLC37 Family.** *Front Chem.* 2018; **6**: 122.
PubMed Abstract | Publisher Full Text | Free Full Text

127. Chou JY, Cho JH, Kim GY, *et al.*: **Molecular biology and gene therapy for glycogen storage disease type Ib.** *J Inherit Metab Dis.* 2018; **41**(6): 1007–1014.
PubMed Abstract | Publisher Full Text

128. Lin SR, Pan CJ, Mansfield BC, *et al.*: **Functional analysis of mutations in a severe congenital neutropenia syndrome caused by glucose-6-phosphatase-beta deficiency.** *Mol Genet Metab.* 2015; **114**(1): 41–45.
PubMed Abstract | Publisher Full Text | Free Full Text

129. Barcelos RP, Stefanello ST, Mauriz JL, *et al.*: **Creatine and the Liver: Metabolism and Possible Interactions.** *Mini Rev Med Chem.* 2016; **16**(1): 12–18.
PubMed Abstract | Publisher Full Text

130. da Silva RP, Nissim I, Brosnan ME, *et al.*: **Creatine synthesis: hepatic metabolism of guanidinoacetate and creatine in the rat *in vitro* and *in vivo*.** *Am J Physiol Endocrinol Metab.* 2009; **296**(2): E256–261.
PubMed Abstract | Publisher Full Text | Free Full Text

131. Edison EE, Brosnan ME, Meyer C, *et al.*: **Creatine synthesis: production of guanidinoacetate by the rat and human kidney *in vivo*.** *Am J Physiol Renal Physiol.* 2007; **293**(6): F1799–804.
PubMed Abstract | Publisher Full Text

132. MacParland SA, Liu JC, Ma XZ, *et al.*: **Single cell RNA sequencing of human liver reveals distinct intrahepatic macrophage populations.** *Nat Commun.* 2018; **9**(1): 4383.
PubMed Abstract | Publisher Full Text | Free Full Text

133. Li W, Wang Y, Zhao H, *et al.*: **Identification and transcriptome analysis of erythroblastic island macrophages.** *Blood.* 2019; **134**(5): 480–491.
PubMed Abstract | Publisher Full Text | Free Full Text

134. Scott CL, Guilliams M: **The role of Kupffer cells in hepatic iron and lipid metabolism.** *J Hepatol.* 2018; **69**(5): 1197–1199.
PubMed Abstract | Publisher Full Text

135. Perez-Riverol Y, Csordas A, Bai J, *et al.*: **The PRIDE database and related tools and resources in 2019: improving support for quantification data.** *Nucleic Acids Res.* 2019; **47**(D1): D442–D450.
PubMed Abstract | Publisher Full Text | Free Full Text

Open Peer Review

Current Peer Review Status: ? ✓

Version 1

Reviewer Report 29 July 2020

https://doi.org/10.21956/wellcomeopenres.17617.r39501

✓ **Luca Cassetta**
University of Edinburgh, Edinburgh, UK

Jeffrey Pollard
College of Medicine and Veterinary Medicine, University of Edinburgh, Edinburgh, EH16 4TJ, UK

A very useful proof of principle paper and a useful proteomic atlas of 2 important mouse macrophage subsets, peritoneal and splenic red pulp ones.

The paper itself is well written, the data are presented in a nice and clear way. It has an enormous amount of information and thus is mainly a resource paper but of great value to the macrophage community. The quantitative nature of the proteomics is a major bonus. Undoubtedly it should be published more or less as is but with a few modifications as suggested below.

Main comments:

1. The authors should acknowledge that the macrophages were isolated in slightly different ways, one with collagenase digestion. This can remove surface markers thus creating an artificial difference. This doesn't reduce the papers value but is just a cautionary note.

2. It should be recognised that comparisons or the CSF1 receptor are very difficult as 90% of this protein is in a cryptic pool and not on the surface – further this receptor is down-regulated by CSF1 ligand thus the density reflects signalling to some degree. Thus, unless the cells are permeabilised the comparison with mRNA levels are not justified. Similarly, CSF1 is usually not made by macrophages (minimal transcripts in the paper) but is internalized continuously on the receptor and thus the detected protein probably reflects receptor activity. Similar problems can be cause by the phagocytic nature of these cells are found for other proteins as noted for the presence of erythrocyte proteins. This again is not to attack the validity of the paper but just that some cautionary notes should be added for the interpretations.

3. The paper would be improved by adding more text in the figure legends and explain a bit better the figures.

Example: Figure 3B, please explain in the legends the meaning of the dotted coloured lines, it is present in the text but figures should be self-explanatory.
Same for figure 2A-D, there are P and S values, not explained in the fig legends.

4. Flow cytometry experiments reported in Fig 3C and 4B and D. How many replicas were performed, can you run statistical analysis on these data?

Is the work clearly and accurately presented and does it cite the current literature?
Yes

Is the study design appropriate and is the work technically sound?
Yes

Are sufficient details of methods and analysis provided to allow replication by others?
Yes

If applicable, is the statistical analysis and its interpretation appropriate?
Yes

Are all the source data underlying the results available to ensure full reproducibility?
Yes

Are the conclusions drawn adequately supported by the results?
Yes

Competing Interests: Both Dr Cassetta and I are co-founders in Macomics a macrophages immunoonclogy company. However, there are no conflicts of interest with this paper.

Reviewer Expertise: Macrophage biology

We confirm that we have read this submission and believe that we have an appropriate level of expertise to confirm that it is of an acceptable scientific standard.

Reviewer Report 28 July 2020

https://doi.org/10.21956/wellcomeopenres.17617.r39500

?

Camille Bleriot
Agency for Science, Technology and Research (A*STAR), Singapore Immunology Network (SIgN), Singapore, Singapore
Florent Ginhoux

Agency for Science, Technology and Research (A*STAR), Singapore Immunology Network (SIgN), Singapore, 138648, Singapore

This report by Nagala & Crocker aims at comparing the proteome of murine splenic red pulp and peritoneal macrophages. Briefly, authors have sorted and profiled these two macrophage populations by using high-resolution quantitative proteomics to gain insights into the functions of these two subsets. The report constitutes a solid but simple resource for the community, confirming what is already published. One could argue about the relevance of the study as an extensive catalog of differentially expressed proteins and hypotheses concerning their biological functions. The flow cytometry validation is undoubtedly important here but the biological relevance is questionable as validation is lacking for the biological relevance of the findings. Also, readers could ask about the choice of the authors to have targeted these two populations. Basically, ones could compare one by one virtually all macrophage populations *i.e*microglia vs. Kupffer cells or alveolar macrophages vs. heart macrophages and obtain a similar study. The underlying question is to decide if this kind of catalog deserves a publication in itself or if it should be reported as a publicly available database.

Few more comments below:

- RBC are lysed for splenic cell preparation but not for peritoneal ones. Even if these are standard procedures, it might artificially induce the aged/damaged erythrocyte recycling program. Do authors have check this with non-lysed samples?

- Page 8: “Other TLRs were expressed at similar levels in both tissue Mφs (Figure 3A and Figure 4A, B)”. No TLR are displayed on Figure 3A.

- Figure 3C is not so relevant as data are already reported in Figures 3A and B. Similarly, there are often the same data reported on different panels.

- What is MF on figures 4A & B? Is it the mean fluorescence intensity recorded by flow cytometry? It seems to not fit with the protein expression data and the plots from figures 4B & D. Authors should clarify this.

- Page 11: “This suggests that PM may be capable of converting vitamin A to RA and that the omentum may not be required for this step as proposed by Okabe (Okabe 2014)” typo, the ref should be included as others.

Is the work clearly and accurately presented and does it cite the current literature?
Yes

Is the study design appropriate and is the work technically sound?
Yes

Are sufficient details of methods and analysis provided to allow replication by others?
Yes

If applicable, is the statistical analysis and its interpretation appropriate?
Yes

Are all the source data underlying the results available to ensure full reproducibility?
Yes

Are the conclusions drawn adequately supported by the results?
Partly

Competing Interests: No competing interests were disclosed.

Reviewer Expertise: Immunology, Macrophage Biology

We confirm that we have read this submission and believe that we have an appropriate level of expertise to confirm that it is of an acceptable scientific standard, however we have significant reservations, as outlined above.